NTNU – Trondheim
Norwegian University of
Science and Technology

TFY4510 - Physics, Specialization Project

Development of Experimental Setups for Measuring Time-domain and Frequency-domain Dielectric Response in Solid Dielectric Immersed in Dielectric Liquids

Elise Otterlei Brenne

Submission date:	December 2016
Supervisor:	Torbjørn Andersen Ve, SINTEF Energy Research
Co-supervisor:	Øystein Hestad, SINTEF Energy Research
Co-supervisor:	Jon Andreas Støvneng, NTNU - Department of Physics

Norwegian University of Science and Technology
Department of Physics

Preface

This report is the result of my work in the course TFY4510 Physics, Specialization Project, autumn semester 2016. It is part of my Master of Science in Applied Physics and Mathematics at Norwegian University of Science and Technology, NTNU. The work presented here is conducted in cooperation with SINTEF Energy Research, and is related to an ongoing research project, *High Voltage Subsea Connectors*. The experimental work was carried out in their laboratories at Gløshaugen with Torbjørn Andersen Ve and Øystein Hestad as main supervisors.

My work this semester has mainly been focused on developing and constructing experimental setups in the laboratories of SINTEF Energy Research, in addition to literature studies as a preparation for work on my Master's thesis spring semester 2016. The idea to the project was developed during my summer internship at SINTEF Energy Research in 2016. This project can be seen as a continuation of the work started then, as presented in the report titled "Measurements of conductivity and dielectric response of PEEK submerged in Midel 7131".

I would like to thank my supervisors Torbjørn Andersen Ve and Øystein Hestad, researchers at SINTEF Energy Research, for valuable help and advice throughout the semester. Also, I would like to thank my supervisor Jon Andreas Støvneng at the Department of Physics, NTNU, and Dag Linhjell, researcher at SINTEF Energy Research for helpful discussions and assistance in the experimental work.

Trondheim, December 20, 2016

Elise Otterlei Brenne

Abstract

Subsea connectors are advanced power cable terminations, considered to be critical components for subsea oil- and gas processing facilities. A combination of solid and liquid insulation material is used in the connector. In order to design reliable connectors, knowledge about how the materials affect each other's electrical properties is essential.

In this project, an experimental setup has been developed for measurements of the dielectric response in time domain and in frequency domain of the polymeric dielectric PEEK (polyether ether ketone) immersed in the synthetic ester Midel 7131, a dielectric liquid. The main challenge in the development process was a high bias current, appearing when Midel was present in the measurement system. The bias current was reduced to a satisfactory level by improving the guarding and shielding of the measure electrode and measuring cable.

A proof of concept was provided by conducting preliminary time-domain measurements and compare the results to measurements performed in air. The results indicate that Midel increases the electrical conductivity of PEEK. The field dependency of the conductivity seems to decrease compared to PEEK in air.

In addition, the construction of an experimental setup for measurements of dielectric response at elevated pressures was started.

Contents

Chapter 1

Introduction

Subsea connectors are considered to be critical components in power transfer systems for subsea oil- and gas processing facilities. A connector is an advanced cable termination, connecting the power cables to the equipment on the seabed. Today, 12 and 24 kV AC subsea connectors are available. Due to an increase in demand for electrical power and longer step-outs, high voltage, low frequency AC and DC connectors must be developed. Obtaining essential knowledge and criteria to design such connectors is the main objective of an ongoing project[1] at SINTEF Energy Research. The work presented in this report is part of this process.

In high voltage subsea connectors, a combination of solid and liquid insulation is used. One possible material combination is the polymeric dielectric PEEK (polyether ether ketone) and Midel 7131, a synthetic dielectric liquid (Appendix A and Appendix B, respectively). Previously, research has been done on each of these materials separately[1, 2]. No published work has been found on the combination of the two. The main objective of this project has therefore been to develop an experimental setup for studying how the electrical properties of PEEK is affected by Midel. Specifically, the setup is designed for measurements of dielectric response of a sample of PEEK immersed in the liquid. From the dielectric response, the electric conductivity and permittivity of the material can be found. These are central parameters for the field distribution in the dielectric, directly related to the reliability of the material for insulation applications. Preliminary measurements were conducted to provide a proof of concept, demonstrating the adequacy of the setup.

On the seabed, the connector will be subjected to a high hydrostatic pressure. How pressure affects the electrical properties of the insulation materials is therefore another important aspect to consider.

---

[1] http://www.sintef.no/projectweb/power-insulation-materials/

Construction of a second experimental setup for studying this effect has therefore also been part of the work carried out this semester. The completion of this setup will be carried out in future work.

The rest of the report is organized as follows. Chapter 2 gives an introduction the physics behind the electric conductivity and dielectric response of a material. In the first part of Chapter 3, an experimental setup for measurements on PEEK in air is presented. This is the base for the development process leading to the final setup for measurements on PEEK in Midel, described in detail in the second part of the chapter. The last part contains a summary of the work done on the setup for measurements at elevated pressures. In Chapter 4, results from preliminary measurements on PEEK in Midel are presented and compared to previous measurements in air.

Chapter 2

Theory

How a dielectric material responds to an applied electric field is called *dielectric response*. We will in this chapter outline this concept, looking specifically at how a dielectric behaves in time-domain as a DC step voltage is applied. The Fourier transform takes us to the frequency-domain, where the application of AC voltage at a range of frequencies can be treated. From the dielectric response, many material properties can be found, including electric conductivity and permittivity.

2.1 Electrical Conductivity in Polymers

Electrical conductivity is an intrinsic property of a material, quantifying how well an electrical current can flow through it. For an insulating polymer, this value is naturally very low, e.g. at the order of 10^{-14} S/m for polyether ether ketone (PEEK)[3]. The conductivity σ is defined by the current density J created by an electrical field E, as given by Ohm's law,

$$J = \sigma E. \tag{2.1}$$

For a "linear" or "ohmic" material, σ is constant with respect to field strength. The current density will then vary linearly with the applied electric field.

In general, conduction of electric current may occur through movement of charge carriers like positive and negative ions, electrons and holes[4]. A hole represents the vacancy of an electron, carrying an equivalent positive charge. The total conductivity can be written in terms of the charge q, mobility μ and concentration n of each species i[5],

$$\sigma = \sum_i q_i \mu_i n_i. \tag{2.2}$$

The mobility is defined as the average of the charge carries drift velocity per unit electrical field,

$$\mu = \frac{\langle v \rangle}{E} = \frac{qt'}{m}. \tag{2.3}$$

The last term originates from the Drude model[6], where t' is the average time between collisions as the carrier move through the material and m is its mass. With no electrical field present, the charge carriers are likely to drift in any direction, with a velocity averaging to zero. However, electro-diffusion of ions can also contribute to conduction. The essence of this transport process is diffusion, in addition to migration of ions in a self-consistent electric field[7]. If the concentration of ions is not even throughout the material, ions will move from a region of high concentration to a region of lower concentration. An electrical field is created around each of the ions to maintain electroneutrality in the material. Oppositely charged ions will repel each other and ions of like charge will attract each other.

For an insulating polymer, the concentration of conducting electrons is very low. To explain this, one can look to *energy band theory* (see text books on solid state physics, e.g. [8]). This theory was originally developed to explain the conductivity of crystalline materials, but does to some extent transfer to polymers[6]. To move an electron from the valence band to the conduction band, and hence contribute to electrical conduction through the material, an energy corresponding to the width of the band gap is required. This energy is high for most polymers, for instance 8.8 eV for polythylene (PE)[9]. Consequently, the contribution from electrons to the conductivity of an insulating polymer is very low.

The conductivity calculated from the concentration of electrons in the polymer is however always lower than the measured value of the conductivity. This is because ions are always present in the polymer, originating from impurities in the material, for example absorbed water or contamination from the production process. The mobility of the ions is affected by the sample morphology. A polymer with a high degree of crystallinity has a lower amount of free volume for the ions to move in[10].

2.1.1 Temperature Dependency

Free and loosely bound electrons can appear from ionization of the polymer macromolecules induced by heat, electrical field, radiation or other factors[11]. The temperature dependence of electrical conductivity is described by an empirical Arrhenius equation,

$$\sigma = A\exp(\frac{-E_\sigma}{kT}). \tag{2.4}$$

Here, T is the temperature and k is Boltzmann's constant. A is an empirical factor, constant or with a weak temperature dependency, and E_σ is the activation energy for the thermally activated charge carries transport process[12]. The Arrhenius relation is valid in a wide temperature range, but with different values for the pre-exponential factor and the activation energy for different temperature intervals. For instance, different values are needed to describe the conductivity above and below the glass-liquid transition temperature T_g (amorphous region) or melting temperature T_m (crystalline region).

2.2 Polarization

When an electric field is applied across a dielectric material, it causes permanent dipoles to rotate and temporary dipoles to be induced in the direction of the field. This effect is called polarization. Before application of any electrical field across the dielectric, all dipoles will be randomly oriented due to thermal agitation.

2.2.1 Dipoles and Dielectric Polarization

In a material, two types of dipoles can be present. A *permanent dipole* is the result of a molecule, e.g. HCl, consisting of atoms of considerably different electron affinity. Each atom will end up with a net charge of magnitude q, in this case $H^+ - Cl^-$, and be fixed at a distance l giving rise to a dipole moment $d = ql$. The other type of dipole is an *induced dipole* caused by an external electric field E, slightly shifting the center of charge for the valence electrons and the positive atom core in opposite directions. In this case the dipole moment is proportional to the applied field, $d = \alpha E$, α being the *polarizability* of the molecule. The *dielectric polarization* P is the geometrical sum of all the dipole moments d in the material.

2.2.2 Polarization Mechanisms

There are four main mechanisms contributing to the polarization of a material, namely atomic, ionic, orientation and interfacial polarization. *Atomic* polarization refers to how a temporary dipole moment is induced in each atom of a material, as the negative electron cloud surrounding the positive nucleus is shifted slightly along the direction of the applied field. Similarly, a temporary dipole is induced in an ionic compound as its positive and negative constituents are pulled in opposite directions by the applied electric field. This is referred to as *ionic* polarization. The generic term for these to mechanisms is *displacement* polarization, considered to happen instantly as the electric field is applied. Likewise, upon removal of the electric field, the induced dipole moments disappear immediately[13].

The following two mechanisms are slower processes, called *relaxion* mechanisms. For *orientation* polarization, otherwise randomly oriented permanent molecular dipoles will be rotated to align with the applied field. After removing the field, thermal agitation tends to randomize the alignment again and the net dipole moment goes back to zero[14].

While the above mechanisms are linked to charges within the atoms or molecules themselves, electrical polarisation may also be associated with mobile charge carriers, e.g. electrons, holes or ions[4]. As the perfect insulating material does not exist, all dielectrics has a certain conductivity and an external field may cause the free charge carriers to move. *Interfacial* or *space charge* polarization refers to how these charges may be trapped at interfaces between different materials or in the bulk of the material, locally distorting the electrical field distribution[14]. In the case of a semi-crystalline polymer, the transitions between crystalline and amorphous regions will work as internal interfaces, causing potential walls that may trap charge carriers[5].

2.2.3 Temperature Dependency

A characteristic feature of the displacement polarisation (atomic and ionic) is their relative independence of temperature, due to their interaction being an intramolecular phenomenon[15]. Orientation polarisation, however, involves the inelastic movement of particles, and is strongly temperature dependent[14]. Consider a set of non-interacting, freely floating permanent dipoles in a static electrical field. The average (orientation) dipole moment is then, in the *low field approximation* $dE << kT$, given by

$$\bar{d} = \frac{d^2 E}{3kT},$$

where k is Boltzmann's constant and T the temperature. The proportionality to the inverse temperature reflects the influence of thermal vibrations at higher temperatures, opposing the alignment of the dipoles by the field[15]. Interfacial polarization will also be temperature dependent, as it is related to movement of charged particles in the material, and hence, the conductivity of the material. The temperature dependence of the conductivity is stated in Equation (2.4).

2.3 Dielectric Response in Time Domain

With a geometry resembling a parallel plate capacitor, a uniform electric field E can be applied across a dielectric material. For an isotropic and homogeneous material, the polarization is proportional to the applied electric field,

$$P = \varepsilon_0 \chi E, \tag{2.5}$$

where ε_0 is the vacuum permittivity and χ is the susceptibility of the material. With vacuum between the capacitor plates, a charge density of magnitude $D_0 = \varepsilon_0 E$ will accumulate on the electrodes. If a dielectric is introduced between the electrodes, the total charge density induced will be a sum of the instantaneous free space contribution and the material polarization $P(t)$,

$$D(t) = \varepsilon_0 E + P(t), \tag{2.6}$$

also called *dielectric displacement*.

The polarization of a material will be delayed with respect to the applied field, simply explained by the inertia of the mass that is transferred in the process. The time-dependence is gived by

$$P(t) = \varepsilon_0 \int_0^\infty f(\tau) E(t-\tau)\, \mathrm{d}\tau, \tag{2.7}$$

where $f(\tau)$ is the *dielectric response function* characterizing the response of the dielectric medium to the applied field. In view of its physical significance, we can conclude that

$$f(t) \equiv 0 \quad \text{for } t < 0. \tag{2.8}$$

This reflects the fact that due to the principle of causality, no response to the application of a field can occur before the field is applied. Moreover, as we are only considering materials with no persistent polarization,

$$\lim_{t\to\infty} f(t) = 0. \tag{2.9}$$

With property (2.8) in mind we can extend the lower limit of the integral in Equation (2.7) to $-\infty$, giving a *convolution integral* of $f(t)$ and $E(t)$, with the physical sense that the dielectric has a “memory” of its past history(REF).

A field of strength E_0 applied at $t = 0$ can be expressed as $E(t) = E_0 \cdot u(t)$ where $u(t)$ is the unit step function. With equations (Equations) (2.6) and (2.7) the dielectric displacement then becomes

$$D(t) = \varepsilon_0 E_0 \left[u(t) + \int_0^t f(\tau)\, \mathrm{d}\tau \right] \tag{2.10}$$

The resulting current is then, from Maxwell's equation defining the current density $J(t)$ in terms of the displacement current and of the direct current conductivity σ[15]:

$$J(t) = \frac{\mathrm{d}D(t)}{\mathrm{d}t} + \sigma E_0 \tag{2.11}$$

$$J(t) = \varepsilon_0 E_0 \left[\delta(t) + f(t) \right] + \sigma E_0 \tag{2.12}$$

where $\delta(t)$ is the delta function. The first term is referred to as the *polarization current* $i_p(t)$ and the last term is the steady state current, caused by the flow of free charges through the material. As $t \to \infty$, we have from Equation (2.9) that the current density relaxes towards the steady state direct current, $J_0 = \sigma E_0$. A steady state polarization P_∞ is then reached. Removing the field abruptly, a *depolarization current* $i_d(t)$ can be observed, equal to the polarization current but with opposite polarity, arising from the relaxation of the dipoles back to their original position from before application of the field.

According to Debye, the part of the displacement current originating from one relaxation mechanism will be exponentially decaying with time, with a decay constant characteristic for the specific mechanism[13]. Figure 2.1 shows an illustration of the current through a material with one relaxation mechanism as a DC step voltage is applied.

2.4 Dielectric Response in Frequency Domain

In frequency domain, the *electric susceptibility* $\chi(\omega) = \chi'(\omega) - i\chi''(\omega)$ describes the response of a dielectric material to a harmonic field at frequency w, with i being the imaginary unit. It is defined as the Fourier transform of the respons function $f(t)$, and is a complex quantity, reflecting the lag in polarization with respect to the driving field. A Fourier transform of the convolution integral in Equaiton (2.7) yields

$$P(\omega) = \varepsilon_0 \chi(\omega) E(\omega) \tag{2.13}$$

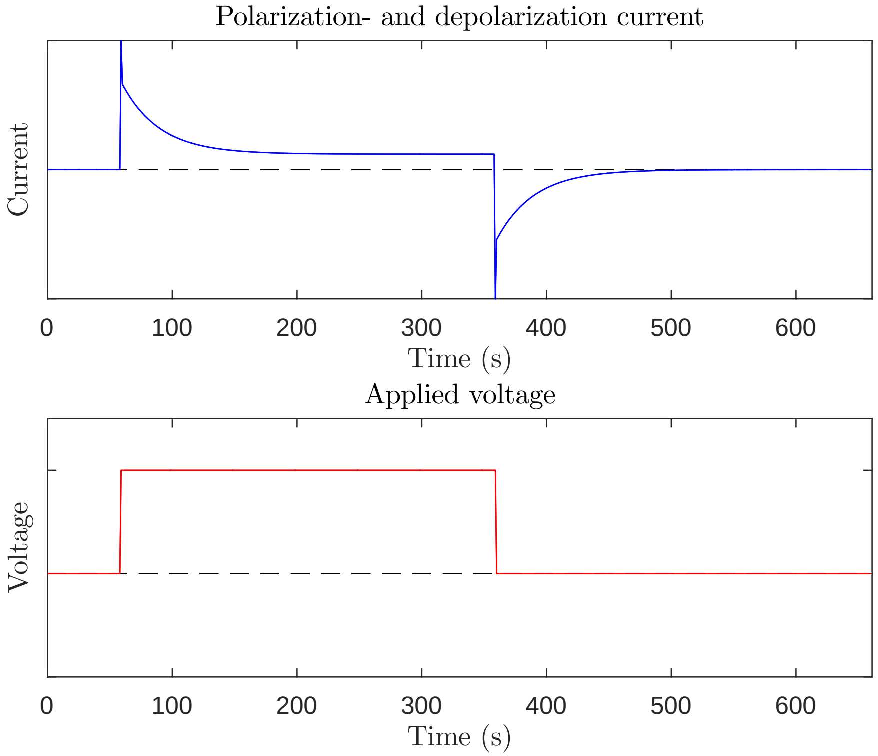

Figure 2.1: An illustration of the current through a material with one relaxation mechanism as DC voltage is applied at $t_1 = 60\,\mathrm{s}$ and removed at $t_2 = 360\,\mathrm{s}$. The spikes in the current density seen at application and removal of the field is due to the instantaneous displacement polarization. Before the field is removed, the current relaxes towards a value proportional to the direct current conductivity.

where $P(\omega)$ and $E(\omega)$ is the Fourier transform of the time-domain polarization and electric field, respectively. The Fourier transform of Equation (2.6) results in

$$D(\omega) = \varepsilon_0 E(\omega) + P(\omega) = \varepsilon_0(1+\chi(\omega))E(\omega) = \varepsilon(\omega)E(\omega), \tag{2.14}$$

defining the complex quantity $\varepsilon(\omega) = \varepsilon'(\omega) - i\varepsilon''(\omega)$ as the frequency dependent *dielectric permittivity* of the material. Combining this with the Fourier transform of Equation (2.12), the following expression for the current density is obtained,

$$J(\omega) = \sigma E(\omega) + iwD(\omega) = \left[\sigma + iw\varepsilon(\omega)\right]E(\omega). \tag{2.15}$$

A measuring instrument cannot distinguish the “true” permittivity from the contribution from the DC conductivity. It is therefore convenient to introduce an *effective permittivity*,

$$\tilde{\varepsilon}(\omega) = \varepsilon'(\omega) - i\left[\varepsilon''(\omega) + \frac{\sigma}{w}\right], \tag{2.16}$$

so that $J(\omega) = i\omega\tilde{\varepsilon}(\omega)E(\omega)$.

The imaginary component of the effective permettivity represents the *dielectric loss* of the material, quantifying the amount of energy dissipated in the insulation. *Ohmic dissipation* reffers to the heat generated as charge carriers collide with atoms on their way through the material. The loss therefore depends on the material conductivity σ. The time dependent polarization (relaxation mechanisms) of the material is another source of energy dissipation, expressed by the imaginary permittivity ε''. Knowledge about the permittivity of a material is therefore important in many engineering applications.

2.4.1 Capacitance and Permittivity

Considering a parallel plate capacitor with a dielectric medium between the electrodes, its *capacitance* is defined as the ratio of the charge Q induced on the electrodes and the voltage U applied across,

$$C = \frac{Q}{U}. \tag{2.17}$$

With an electrode area A much bigger than the distance d between them, edge effects can be ignored and the electric field between the electrodes will be uniform and given by $E = U/d$. As described in Section 2.3, the dielectric displacement $D = \varepsilon E$ represents the total charge density induced at the electrodes by the field, so that

$$Q = AD = A\varepsilon E = \frac{A\varepsilon U}{d}, \tag{2.18}$$

which together with Equaiton (2.17) gives the following expression for the capacitance,

$$C = \varepsilon\frac{A}{d}. \tag{2.19}$$

Hence, with a well-defined geometry of the capacitor, the permittivity ε of the dielectric between the electrodes can be calculated from measurements of the capacitance.

Chapter 3

Experimental Work

The main objective for this project is to develop an experimental setup for measuring the dielectric response in time and frequency domain of a solid dielectric material immersed in a dielectric liquid. The setup will be based on an existing setup for measurements on a solid material in air at atmospheric pressure, as will be presented in Section 3.1. A detailed description of the development process follows in Section 3.2, showing how the original setup was modified to work with the sample immersed in liquid. Section 3.3 provides an overview of the construction of an experimental setup for measurements at elevated pressure.

3.1 The Original Setup

The setup presented in this section is designed by researchers at SINTEF Energy Research. It has previously been used to measure the conductivity and permittivity of PEEK and silicone rubber at temperatures between 30 °C and 90 °C[2, 16]. The equipment used is shown in Figure 3.1.

The setup is designed to measure the dielectric response of a dielectric material in both time and frequency domain. Both methods are based on measuring the current through the bulk of a sample as voltage is applied across it. During measurements, the sample is placed in a test cell as described in Section 3.1.2. The measured currents are very small, in order 10^{-12}–10^{-9} A, and therefore very sensitive to noise from the surroundings. The test cell is therefore placed inside a Faraday cage, as seen in Figure 3.2. The Faraday cage is placed in a climate chamber controlling the temperature.

For measurements in time domain, the measuring circuit in Figure 3.5 is used, measuring the current through the sample as a DC step voltage is applied across it. From this, the conductivity of the material can be calculated. In frequency domain, the circuit in Figure 3.6 is used. Novocontrol, a dielectric spectroscopy instrument, applies AC voltage across the sample at a range of frequencies and measures the current through the sample. From this, the permittivity of the material can be calculated. In Section 3.1.3, the measurement procedures will be explained in more detail to demonstrate the functionality of the setup.

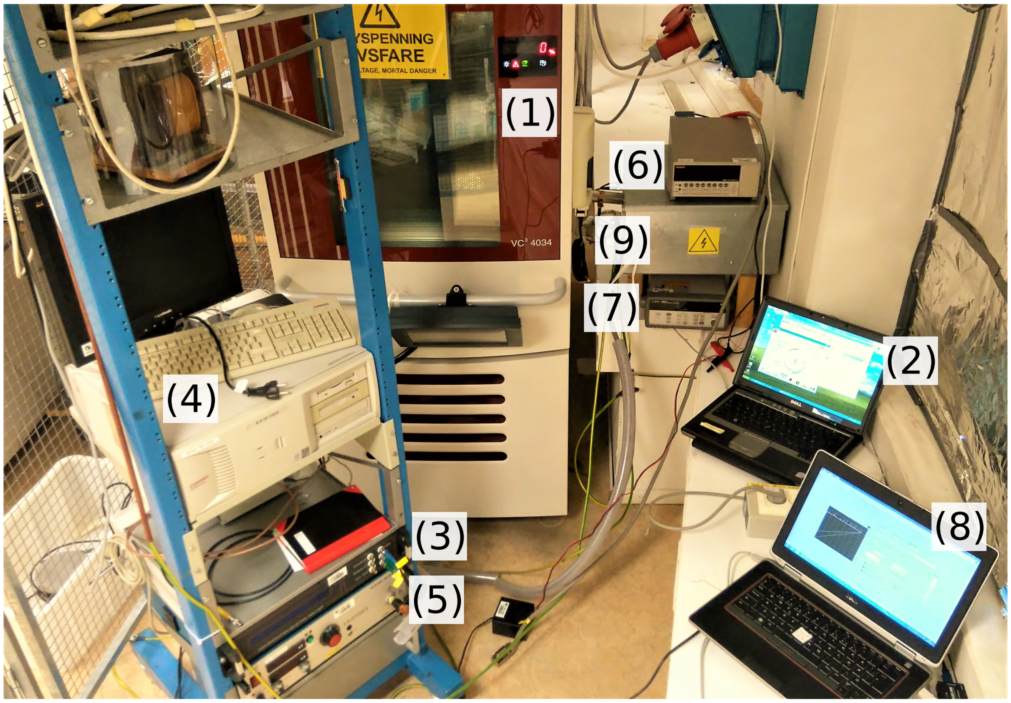

Figure 3.1: Experimental setup for measurements of dielectric response of PEEK in time and frequency domain. The sample is placed inside a climate chamber (1) keeping a stable temperature, controlled by PC (2). For frequency domain measurements, the Novocontrol instrument (3) is connected to the measuring circuit as described in Section 3.1.3.2 and controlled through the PC (4). For time domain measurements, the voltage applied across the sample is provided by the ultra stable HVDC source (5). The current through the sample is measured by a picoammeter (6). The measuring procedure is automated using LabVIEW (PC (8) and Agilent (7)), connecting and disconnecting the voltage source and picoammeter through a relays in the box (9).

3.1.1 Sample Preparation

3.1.1.1 PEEK

The PEEK samples used in this experiment were prepared by Jostein Danielsen Kvitvang[1] in 2015. Each sample is a circular disc with a diameter of approximately 100 mm, cut from larger sheets prepared by the

---

[1] Summer student at SINTEF Energy Research, Electrical Power Technology 2015

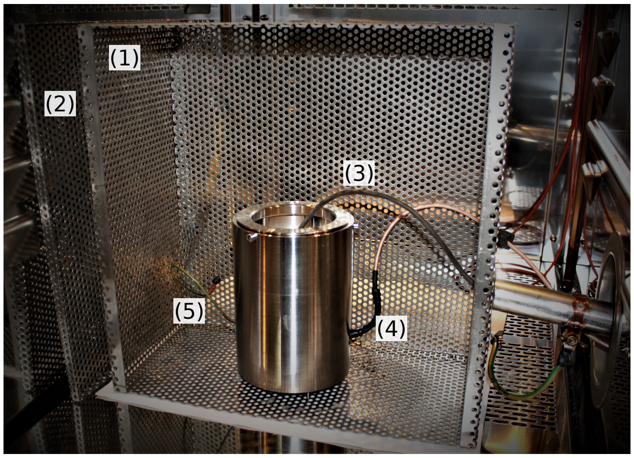

Figure 3.2: Inside the climate chamber. The test cell placed in a Faraday cage (1). During measurements, the lid (2) is put on. Voltage is applied across the sample through cable (3) and the current through the sample is measured by a picoammeter through cable (4). Cable (5) grounds the guard electrode.

manufacturer from VESTAKEEP 3300G (Appendix A). The thickness is 0.25 mm. To ensure good electrical contact between the sample and the electrodes during measurements, the sample has an aluminium coating on both sides as shown in Figure 3.3. Figure 3.3b shows one side of the sample whith the high voltage electrode with a diameter of 65 mm. Figure 3.3a shows the other side of the sample with the 40 mm diameter measure electrode, encircled by the guard electrode. The gap between the guard and measure electrodes is 0.2 mm. The guard electrode is intended to prevent surface leakage current from going around the edges of the sample and reach the measure electrode. Including a guard electrode also ensures the homogeneity of the field at the edge of the measure electrode, moving the fringe effect to the outside edges of the guard electrode.

The samples were dried in a vacuum chamber at 80 °C for three days. The temperature was then turned down to room temperature (25 °C) before opening the vacuum chamber to avoid condensation of impurities from the room air onto the samples. The samples are kept in the vacuum chamber at room temperature until right before measurements.

3.1.1.2 Midel

The Midel was dried for two days in a rotary evaporator where moisture evaporates under reduced pressure. A measurement of the water content of the Midel was then performed by Karl Fisher titration, showing a water content of 5 ppm when taken directly from the rotary evaporator.

(a) Measure electrode and guard electrode. **(b)** High voltage electrode.

Figure 3.3: The to sides of a PEEK sample with aluminium electrodes.

3.1.2 Test Cell

During measurements, the sample is placed in a test cell as shown in Figure 3.4. The test cell is constructed to keep the sample in place and to ensure good contact between the sample and the electrodes. The electrodes, made of brass, aligns with the aluminium coating on the sample. As parts of the test cell might expand at high temperatures, spring coils are placed under the lid of the cylinder to ensure equal pressure on the sample at all temperatures.

3.1.3 General Measurement Procedures

In this section, procedures for measurements of dielectric response in time and frequency domain are presented. Specifically, the procedures described here were followed for measurements on PEEK with the setup in air during summer 2016[17]. The procedures are described in detail because they elegantly describes the functionality of the setup for measurements in air, and also, the intended functionality of the developed setups for measurements in Midel and at elevated pressures.

3.1.3.1 Measuring Dielectric Response in Time Domain

The dielectric response of PEEK in time domain is found by measuring polarization and depolarization currents through a sample as a DC step voltage is applied. A sample is placed in the test cell as described in Section 3.1.2. The test cell is then placed in the Faraday cage inside the climate chamber, as shown in

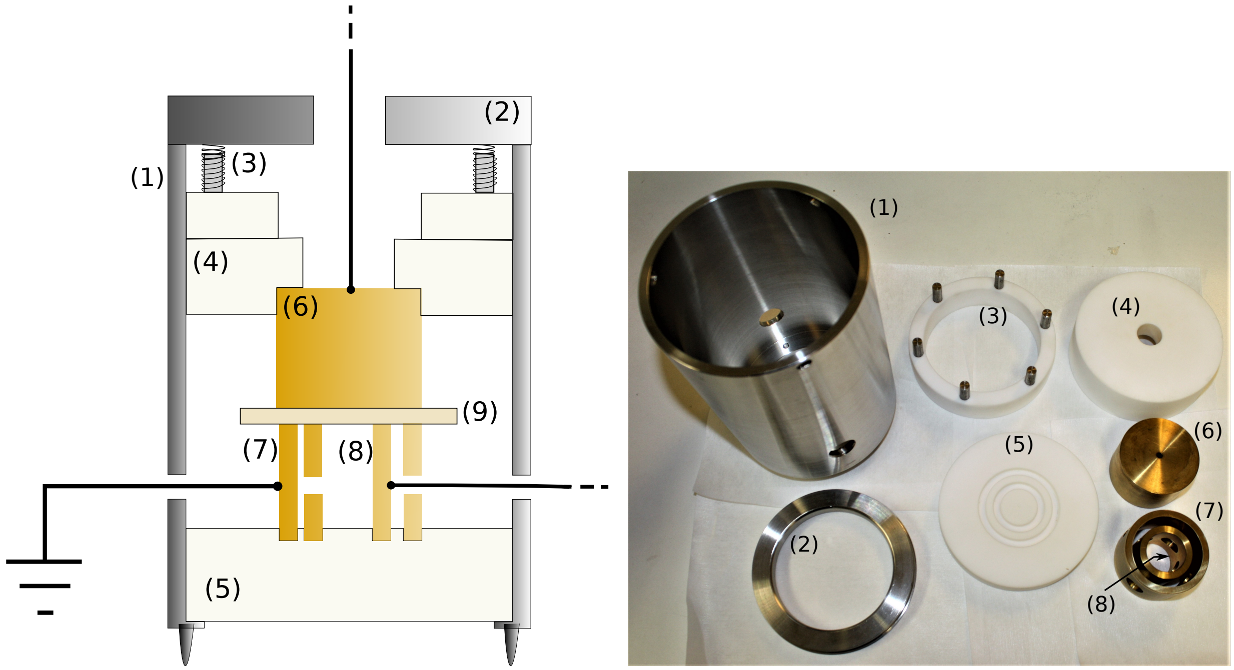

(a) **(b)**

Figure 3.4: The test cell used to ensure good contact between the PEEK sample and the electrodes. Showing (1) cylinder of stainless steel, (2) the lid, (3) PTFE holder with coil springs, (4) and (5) are insulating PTFE holders keeping the electrodes in place, (6) high voltage electrode, (7) guard electrode and (8) measure electrode. In Figure (a), (9) is the sample.

Figure 3.2.

After arranging the cables and setting the temperature of the climate chamber, a delay of minimum 16 hours is set before the measurements are run. This is done to ensure a uniform and stable temperature in the test cell and sample, in addition to warm up the picoammeter and the HVDC source for higher accuracy. Waiting also reduces noise in the measurement circuit due to the triboelectric effect; when cables are moved, or subject to vibration or thermal expansion, charges may be generated between the conductor and the insulator due to friction[18].

The measurement circuit is shown in Figure 3.5. An ultra stable HVDC source is used to apply voltage across the sample and a picoammeter measures the current through the sample. First, noise is measured for 15 minutes. Then, voltage is applied for 1 hour and the polarization current through the sample is measured. Finally, the high voltage electrode is grounded and the depolarization current is measured for 10 hours. A high voltage relay is used to connect and disconnect the HVDC source to the measurement circuit. The input on the picoammeter is short-circuited to ground during switching to avoid high transient currents damaging the instrument. The entire procedure is automated using LabVIEW[2] for voltages

---

[2] National Instruments LabVIEW, a graphical system design platform, `http://norway.ni.com/labview`

1, 2, 3, 4, 5, 6 and 7 kV. From the measured current response, the conductivity of the material can be calculated.

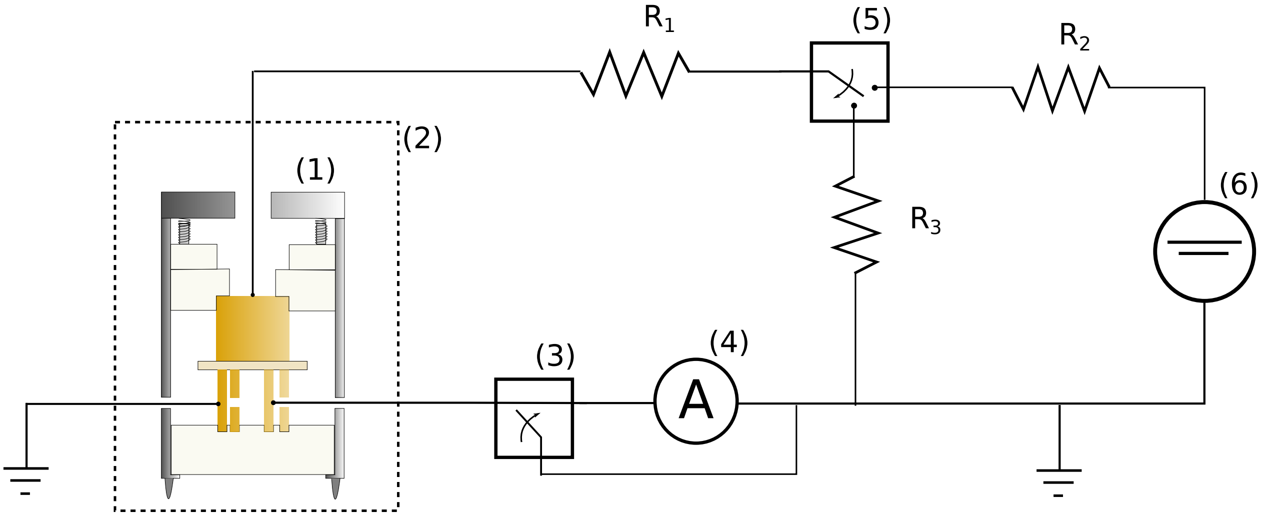

Figure 3.5: A schematic of the conductivity measurement setup, showing (1) test cell with sample, (2) Faraday cage and climate chamber, (3) low voltage short circuit relay, (4) picoammeter, (5) high voltage switch relay and (6) ultra stable HVDC source. $R_1 = 50\,\mathrm{k\Omega}$, $R_2 = 50\,\mathrm{M\Omega}$ and $R_3 = 10\,\mathrm{k\Omega}$.

3.1.3.2 Measuring Dielectric Response in Frequency Domain

The dielectric response of PEEK in frequency domain is measured with Novocontrol, a broadband dielectric spectrometer. As for the conductivity measurements, the sample is placed in the test cell inside the climate chamber, as shown in Figure 3.2, which is set to the desired temperature. The Novocontrol instrument is connected to the test cell and sample as shown in Figure 3.6. A delay of minimum 16 hours is required before starting the measurement, as explained in the section above.

The instrument applies an AC voltage across the sample at a range of frequencies and analyzes the current response. From this, several material parameters can be calculated, including the complex permittivity of the material.

3.1.4 Initial Measurements on PEEK in Midel

During summer 2016, measurements of dielectric response were performed on PEEK with the original setup in air[17], following the procedures described in Section 3.1.3. Then, the first attempt was made to measure the conductivity of PEEK immersed Midel, following the procedure described in Section 3.1.3.1 but at 5 kV and 7 kV only. The temperature was set to 90 °C. The test cell with the sample was placed in

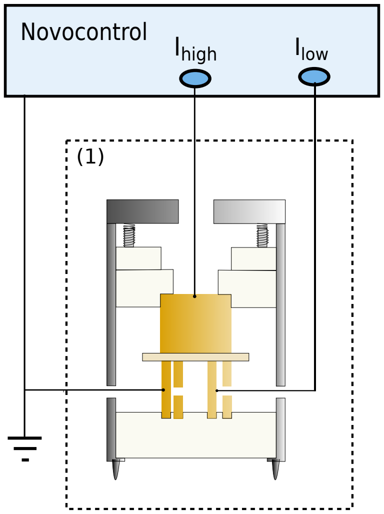

Figure 3.6: A sketch showing how the Novocontrol is connected to the sample in the test cell (2) during measurements of dielectric response in frequency domain. (1) is the Faraday cage and climate chamber.

a container filled with Midel, covering the sample and approximately one centimeter of the high voltage test cell electrode with liquid, see Figure 3.7.

From the measured current response, a value for the *total current* was calculated. This is done by first subtracting an average of the noise measurement in order to remove any DC bias. Then, the polarization and depolarization currents are added pointwise. With ideal guarding, this should leave a signal with contribution only from the direct current conductivity of the material, see Section 2.3. The conductivity is then calculated with Equation (2.1), using an average of total current and the sample geometry described in Section 3.1.1.

Table 3.1 shows the conductivity of PEEK, calculated from the measurements of dielectric response in time domain at 7 kV in air (no. 1) and in Midel (no. 2). An apparent increase in conductivity of 4 orders of magnitude is seen.

To test whether the measured change truly came from changes in the material due to Midel, the same measurements were performed on a sample of polytetrafluoroethylene (PTFE), first in air, then in Midel. PTFE is a well known, essentially chemically inert material absorbing no notable amount of moisture[19]. It is therefore expected that the conductivity of PTFE not should be affected by Midel, and hence, measurements on PTFE in air and in Midel should give approximately similar result.

However, an apparent increase of four orders of magnitude is seen in the conductivity of PTFE when introducing Midel to the system, see measurements no. 3 and no. 4 in Table 3.1. This indicates that the Midel most likely affected the setup itself rather than the sample alone. The increase in the measured current, and hence the calculated conductivity, could be a result of a higher leakage current reaching the

Table 3.1: Results of initial measurements on PEEK and PTFE, in air and in Midel. The temperature is set to 90 °C and the applied voltage is 7 kV. For both materials, an apparent increase of four orders of magnitude is seen in the conductivity when Midel is introduced to the system.

No. (#)	Date	Average total current I_{avg} (A)	Conductivity σ (S/m)	Comment
1.	20160704	8.03×10^{-12}	9.13×10^{-16}	PEEK in air
2.	20160714	7.68×10^{-10}	8.74×10^{-12}	PEEK in Midel
3.	20160817	2.31×10^{-13}	6.37×10^{-17}	PTFE in air
4.	20160819	2.86×10^{-9}	7.88×10^{-13}	PTFE in Midel

measure electrode or the measuring cable. An increase in leakage current is likely as the conductivity of Midel is approximately a factor 10^5 higher than the conductivity of air.

To be able to measure any significant change in PEEK due to Midel, a low noise level, and an either absent or consistently repeatable bias current is required. A process was therefore started to try to reduce the bias current measured in Midel to an acceptable level.

3.2 Setup Developement

This section describes the process of adapting the setup for measurements in air to work for measurements on a sample of PEEK immersed in Midel. Incremental changes have been made, mainly to the measuring cable connecting the measure electrode to the picoammeter. For each iteration, a measurement on PTFE was performed to monitor how the adjustments made to the setup were affecting the measured current. A value for the average total current was calculated to compare the different iterations, as explained in Section 3.1.4. A detailed description of the main changes will be presented in Sectrion 3.2.4, along with a brief comment on the result.

As mentioned, it is assumed that the PTFE sample is not affected by the Midel. The increase in measured current on PTFE is therefore assumed to arise from leakage current going through the Midel rather than from changes in the material itself. Therefore, the main focus during the development process was on improving the guard and the measuring cable screen, to reduce the contribution from the leakage current to the measured current. Ideally, with proper shielding of the measuring cable and electrode, it should be possible to get the same result for measurements in air and in Midel. The goal of the process, however, is to be able to measure changes in the conductivity of PEEK due to Midel. A level of bias current well below the measured current of PEEK in air is therefore satisfactory. This will be discussed further in Chapter 4.

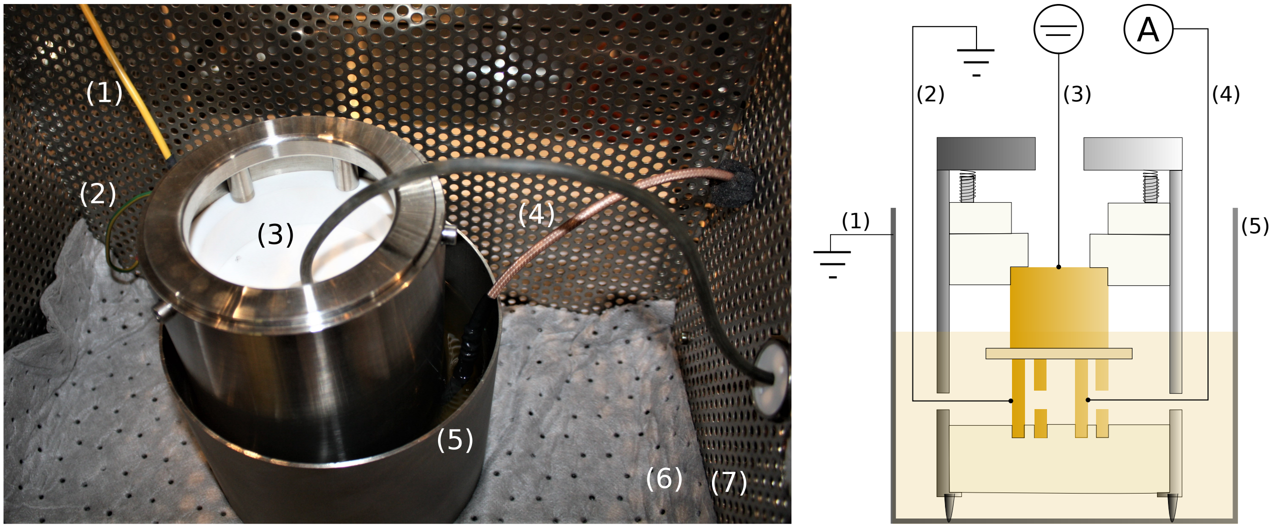

(a) **(b)**

Figure 3.7: The setup used during the development process. The container (5) is filled up with Midel so that the sample inside the test cell is immersed in the liquid. Cable (1) grounds the container and the test cell, (2) grounds the guard electrode, (3) connects the high voltage electrode to the HVDC source and (4) connects the measure electrode and the picoammeter. In figure (a), the padding (6) absorbs oil spill inside the Faraday cage (7).

Figure 3.7 shows the setup used for this process, with the sample and test cell placed in a container filled with Midel. The sample and approximately one centimeter of the high voltage electrode is covered with liquid. As for measurements in air, the test cell is placed in a Faraday cage inside a climate chamber. The equipment used is showed in Figure 3.1 and the measuring circuit is sketched in Figure 3.5. The measurements are performed as explained in Section 3.1.3.1, but at 7 kV only. The temperature is set to 90 °C.

3.2.1 Sample Preparation

The PTFE sample used during the development process is a circular disc with a diameter of approximately 100 mm. The thickness is 1 mm. For the first iterations the sample had no aluminium coating. In iteration no. 5, aluminium electrodes are applied on one side of the sample, see Figure 3.8, following the process described below.

(a) Measure electrode and guard electrode.

(b) High voltage side, has no aluminium coating.

Figure 3.8: Example of a PTFE sample with aluminium electrodes on one side only.

3.2.1.1 Aluminium coating

An aluminium coating was applied on the PTFE samples by the use of a vacuum evaporator. The samples were conditioned in a vacuum chamber for three days at 80 °C before starting. This drastically reduces the time it takes to evacuate the bell jar.

Three samples were placed in the bell jar, and a small piece of aluminium was placed in a tungsten wire basket below the samples. The bell jar was then evacuated by a rotary pump and a diffusion pump. The tungsten wire was heated by passing a current through it, causing the aluminium to melt and evaporate. Reaching the cool surface of the sample, the aluminium condensed and after approximately one minute a uniform well-covering layer had been deposited. To prevent oxidation of the aluminium, the samples were left to cool down under vacuum for about one hour.

Comparing Figure 3.3a and Figure 3.8a, the aluminium coating on the PTFE sample appears to be more “fuzzy” than the coating on the PEEK sample. This indicates that some oxidation has taken place. This might be a result of poor vacuum quality, too low deposition rate or that the samples were not cooled down enough before being removed from the bell jar and exposed to air. However, the result is considered to be good enough as it sticks well to the PTFE. This will be the crucial factor to ensure good electrical contact between the sample and test cell electrodes.

3.2.2 Changes to Measure Electrode and Guard Electrode

As can be seen in Figure 3.4b, the measure and guard electrode are hollow cylinders, and have holes in the side to let Midel fill the space under the sample. However, test showed that after pouring Midel into the container with the test cell, small pockets of air were trapped under the sample. Therefore, small grooves were made on the top surface of the guard- and measure electrodes, as can be seen in Figure 3.9. New test showed some improvement, but some air was still left under the sample. The solution to this was to postpone the assembly of the test cell until after filling the container with Midel. The sample could then be placed on top of the electrodes after the space between them was filled with liquid.

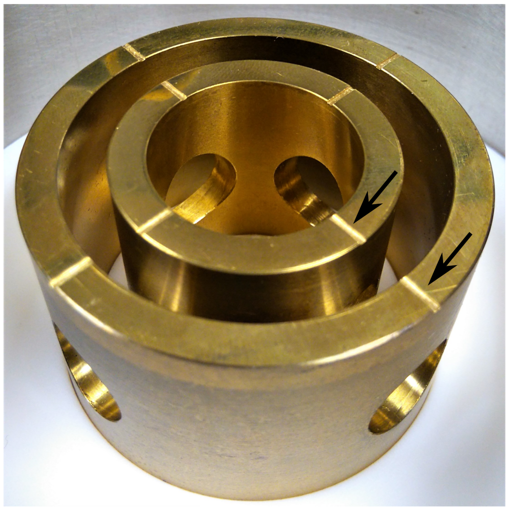

Figure 3.9: Small grooves on the top surface of the measure and guard electrode, so that Midel can fill the space within the electrodes, below the sample. Four grooves on each electrode.

3.2.3 Verifying Electrical Contact Between Sample and Electrodes

Assembling the test cell while submerged in Midel solves the problem with air filling the space within measure and guard electrode. However, this leads to a layer of Midel between sample and electrodes. To find out whether the Midel film had any impact on the electrical contact between the sample and electrodes, a test investigating the contact resistance was performed.

The HV side of a PEEK sample has an aluminium coating with a diameter covering both guard and measure electrode. Putting the sample on top of the guard and measure electrode with this side down and the HV test cell electrode on top for pressure, a multimeter was used to measure the resistance between the two electrodes. This was done several times with clean electrodes and sample, and also with a layer of Midel in between the electrodes and the sample.

The resistance was found to vary considerably with how much pressure was applied when putting the HV electrode in place, from 0.5–10 Ω. No significant difference was noted between the test with Midel present and not, indicating that the effect of a thin Midel film on the electrical contact between the sam-

Table 3.2: Results of measurements on PTFE in Midel. Letters in parentheses refers to the different versions of the measurement cable, as illustrated in Figure 3.10.

No. (#)	Total current (A)	Cable	Comment
1.	2.86×10^{-9}	(a)	With PEX heatshrink tubing.
2.	4.72×10^{-11}	(b)	With PTFE heatshrink tubing.
3.	4.76×10^{-11}	(b)	No change, one month later.
4.	9.96×10^{-12}	(c)	Cable screen overlapping banana plug.
5.	3.50×10^{-11}	(d)	Cable screen connected to guard electrode. Copper tape covering guard electrode holes.
6.	4.11×10^{-11}	(d)	Aluminium foil as guard beneath measure electrode.
7.	5.74×10^{-11}	(d)	Aluminium foil removed. Aluminium electrodes applied on sample.
8.	5.86×10^{-11}	(d)	Less Midel in the container, filled up to just below the sample, above the cable.
9.	7.12×10^{-14}	(d)	Less Midel, filled up to just below the cable.
10.	1.90×10^{-10}	(e)	Cable with no screen.
11.	2.01×10^{-12}	(f)	Cable connected under test cell.
12.	9.22×10^{-13}	(f)	No change
13.	8.27×10^{-13}	(f)	No change

ple and test cell electrodes was negligible.

3.2.4 The Iterative Development Process

As will be discussed in more detail later, the main hypothesis for the high apparent bias current has been that some current goes around the edges of the sample and reaches the measurement cable or the measure electrode, avoiding being picked up by the guard. The main adjustments to the setup has therefore been to try to improve the guarding and to better screen the measuring cable.

The average total current calculated from the measurements on PTFE in Midel are listed in Table 3.2, numbered in chronological order. In the following, the measurements will be referred to with the listed number, and the main changes to the measurement setup will be described.

1. Heatshrink tube replaced and extra screen added

To begin with, the measurement cable had a polyolefin (PEX) heatshrink tube covering a lengthening of the cable screen and parts of the banana plug, see Figure 3.11a. Checking the heatshrink tube after the first measurements in Midel, it was clear that it had absorbed Midel, which potentially could change

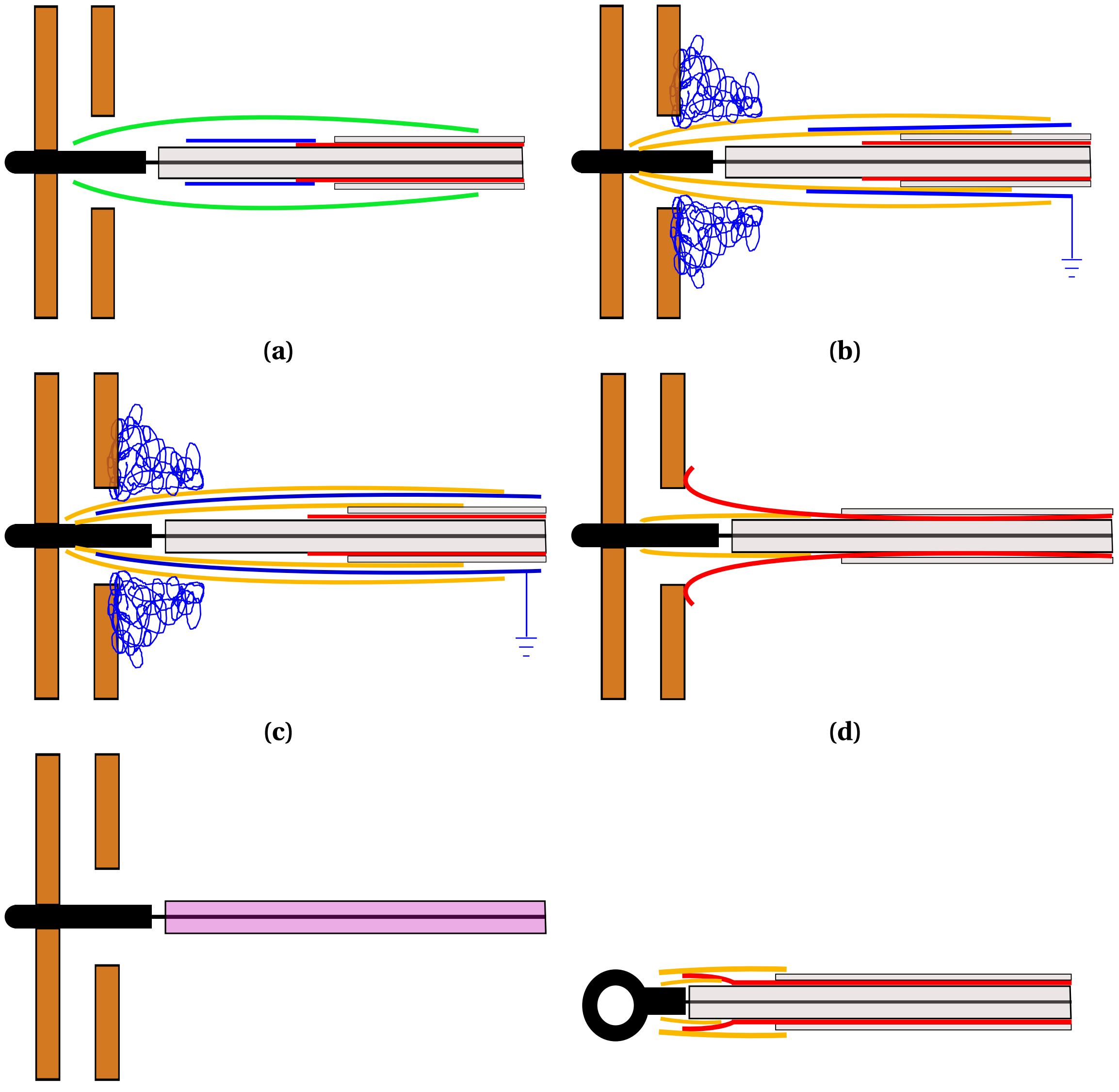

(a) (b)

(c) (d)

(e) (f)

Figure 3.10: Sketches of the different versions of the measurement cable tried during the development process. The green lines represents PEX heatshrink tube, yellow is PTFE heatshrink tube, red is the original cable screen, blue is additional screens made out of fine-meshed metal netting. Cable (e) has a rubber-based insulation while the rest is a coax-cable with PTFE insulation.

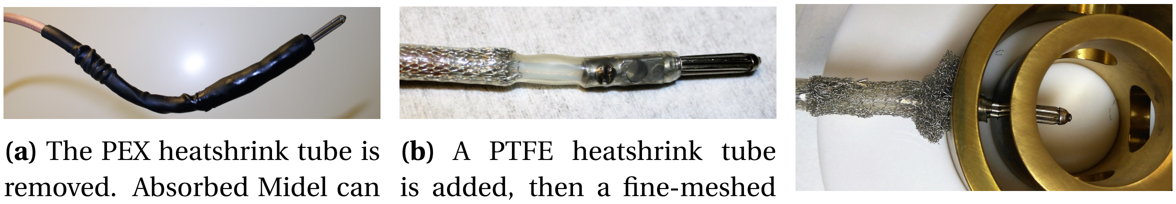

(a) The PEX heatshrink tube is removed. Absorbed Midel can be seen reappearing on the surface after cleaning.

(b) A PTFE heatshrink tube is added, then a fine-meshed metal screen, then a PTFE heatshrink tube.

(c) An additional screen fills the hole in the guard electrode. .

Figure 3.11: Cable modification, first iteration. See Figure 3.10a and 3.10b.

its properties. The first step was therefore to replace the PEX heatshrink tube with one made of PTFE. In addition, an outer screen was added to provide extra protection against leakage currents, see Figure 3.11b. An additional screen was put on to fill the gap between measuring cable and guard electrode, see Figure 3.11c.

Result. This fix resulted in a great improvement, with a decrease in the total current by two orders of magnitude, from 2.86×10^{-9} A to 4.72×10^{-11} A (measurement no. 1 and 2 in Table 3.2). A plot of the measured current before and after this first iteration is shown in Figure 3.12a and Figure 3.12b, respectively. The polarization current in the first plot is very unstable. The polarization current in the last plot is much more stable, resembling the theoretical polarization current shape.

2. Lengthening of the cable screen

As can be seen in Figure 3.11(b), the inner cable screen does not cover the last 2 cm before the banana plug. Therefore, the screen was now lengthened to overlap with the plug to ensure that no part of the conductor is unshielded. A PTFE heatshrink tube separates the screen from the banana plug.

Result. The measured current decreased further, from 4.76×10^{-11} A to 9.96×10^{-12} A (measurement no. 3 and 4 in Table 3.2).

3. Cable screen connected to guard, copper tape seals the holes

As leakage current still seemed to find its way past the guard, a different solution was tested, covering the holes in the guard electrode with copper tape, see Figure 3.13b. Small holes were made to let Midel get in. The extra metal netting screen was removed from the measurement cable. Instead, the last 3 cm of the original cable screen was stripped of insulation (see Figure 3.13a) to prevent leakage current from following the measurement cable to the measure electrode.

Result. This solution gave no significant change in the measured current, although a small increase

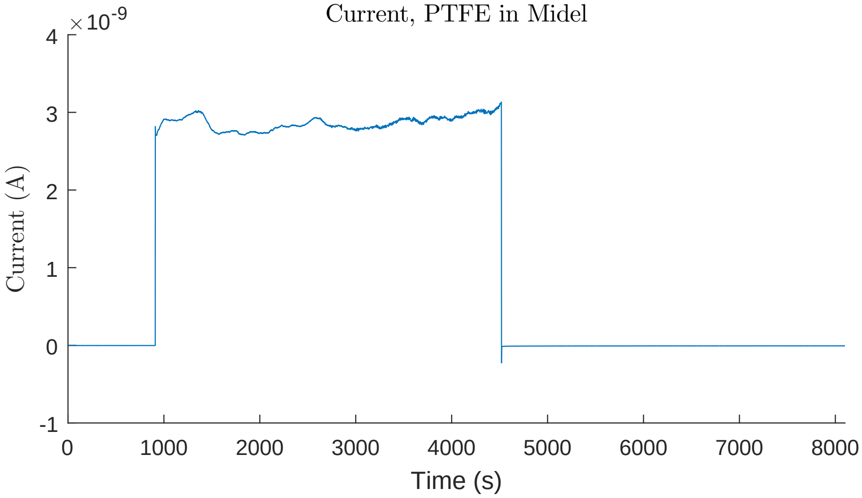

(a) Measured current with PEX heatshrink tube, cable illustration in Figure 3.10a.

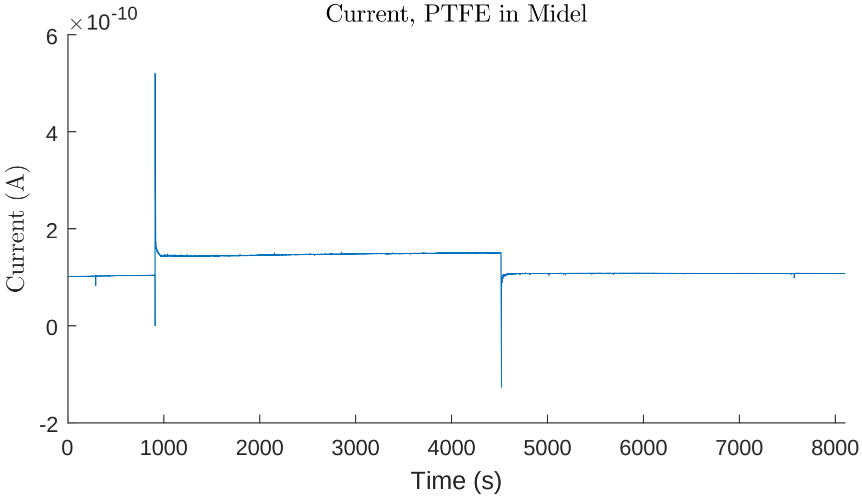

(b) Measured current with PTFE heatshrink tube, cable illustration in Figure 3.10c.

Figure 3.12: Plots of the current from measurements on PTFE in Midel before (figure (a)) and after (figure (b)) the first iteration. A decrease in the total current is seen, in addition to a much more stable polarization current.

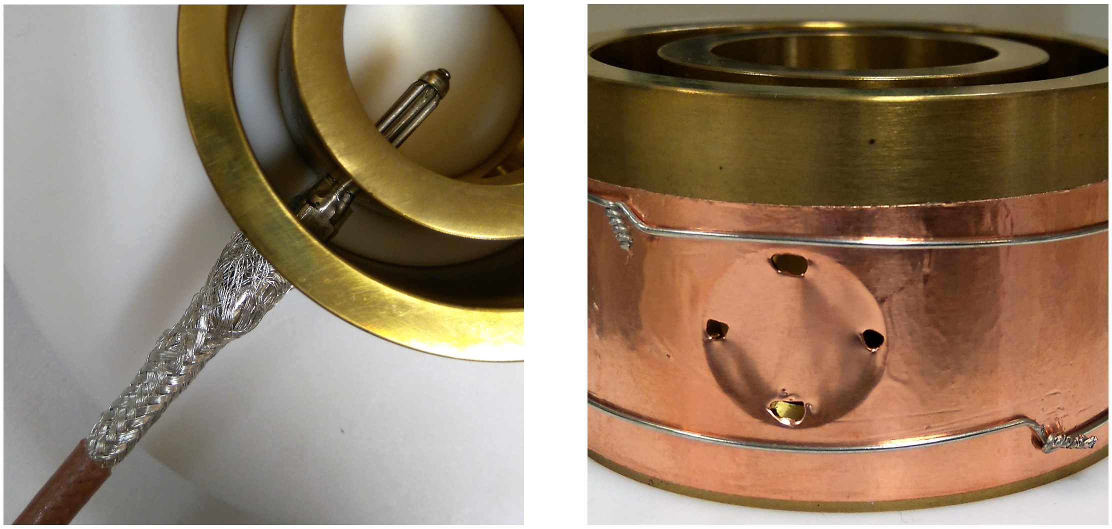

(a) (b)

Figure 3.13: Cable and guard electrode modification, second iteration. Copper tape seals the holes in the guard electrode and the cable screen is in contact with the guard, intended to stop leakage current from passing the guard by following the measurement cable. Illustrated in Figure 3.10d.

is seen compared to the previous measurement, see measurement no. 5 in Table 3.2.

4. Aluminium foil encapsulating the measure electrode

To ensure that no leakage current could reach the measure electrode from underneath, the guard electrode was now wrapped in aluminium foil as seen in Figure 3.14. PTFE plates were used to keep the guard and measure electrode at the same height as illustrated in the figure. This construction did not keep the electrodes perfectly in place, but worked well as a test to see if an encapsulating guard led to any improvement.

Result. See measurement no. 6 in Table 3.2. No significant change in measured current, only a slight increase is seen compared to measurement no. 5.

5. Aluminium coating applied on sample

The aluminium foil in iteration 4 did not improve the guarding, and the PTFE plates made it difficult to keep the electrodes in place. The foil was therefore removed and the electrodes were put back in the original PTFE holder. To improve the contact between the PTFE sample and the test cell electrodes, an aluminium coating was applied on the side of the sample facing down, as described in Section 3.2.1.1.

Result. See measurement no. 7 in Table 3.2. No significant change, but a slight increase in current compared to measurement no. 6.

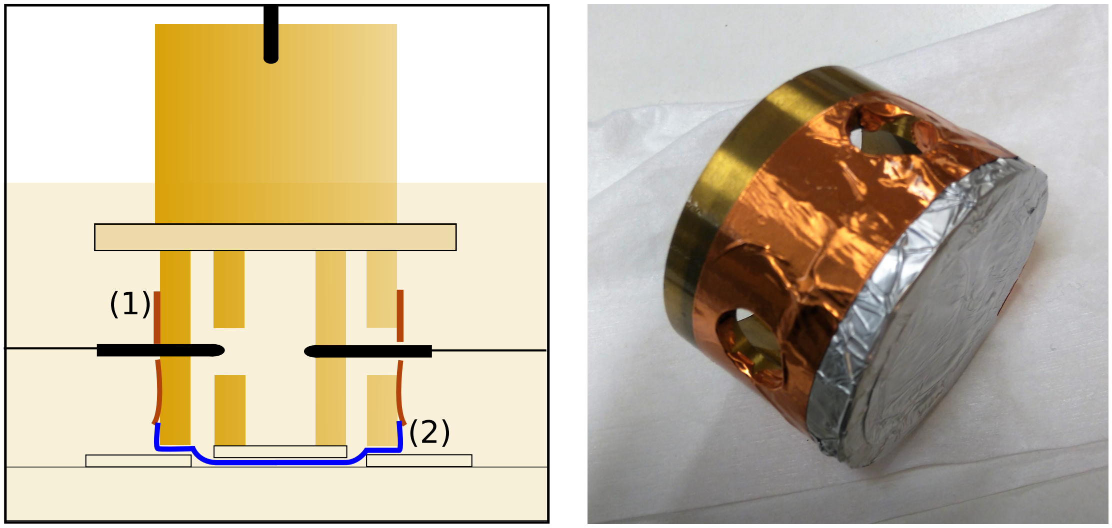

(a) **(b)**

Figure 3.14: Guard electrode modification, fourth iteration. Copper tape (1) seals the holes in the guard and attaches the aluminium foil (2), wrapped around the guard electrode to make sure no leakage current can reach the measure electrode from beneath.

6. Measurement cable connected under test cell

A new approach is tried, connecting the measurement cable under the test cell instead of going in from the side, see Figure 3.15. The banana plug of the measurement cable is replaced with a cable shoe, attached to a bolt going through the PTFE holder and up to the measure electrode. This way, the cable is at a much longer distance from the guard and high voltage electrodes, and is separated from them by the walls of the test cell.

Result. This solution greatly improved the result, reducing the measured current by one and a half order of magnitude, resulting in 2.01×10^{-12} A, see measurement no. 11 in Table 3.2. To confirm the result, two more measurements were performed with no changes made to the setup, see measurement no. 12 and no. 13.

Conclusion

The final measurement on PTFE gave a total current of 8.27×10^{-13} A (Measurement no. 13, Table 3.2). This is one order of magnitude above the level measured for PTFE in air of 2.31×10^{-13} A (measurement no. 3 in Table 3.1), indicating that bias current is still contributing to the measured current. However, for PEEK, the current measured in air is 8.03×10^{-12} A. A bias current level around 1 pA should then be sufficiently low.

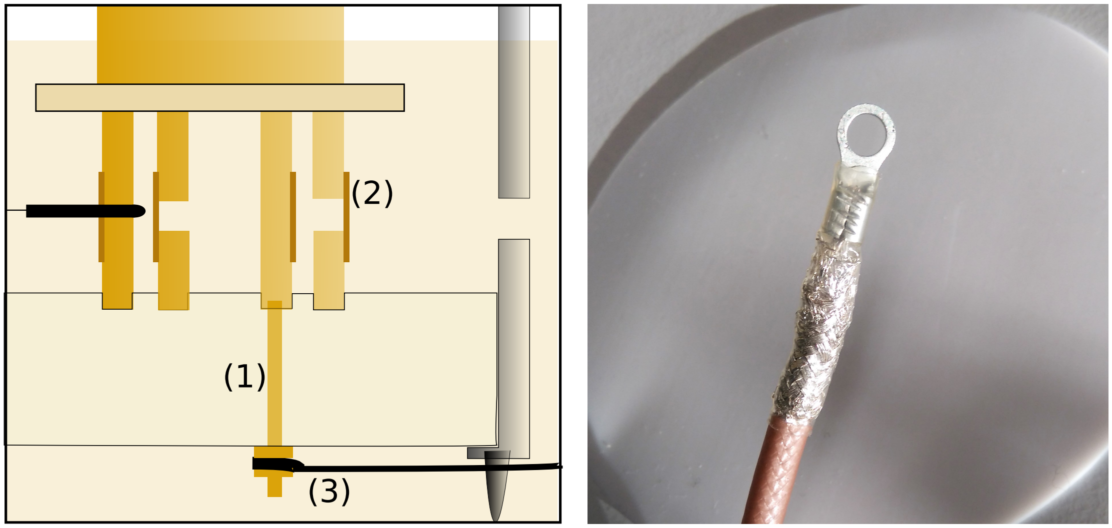

(a) (b)

Figure 3.15: Cable modification, sixth iteration. A bolt (1) is going through the PTFE holder and up to the measure electrode. Copper tape (2) seals the holes in the electrodes. The banana plug of the measurement cable (3) is replaced with a cable shoe, shown in Figure 3.15b.

3.2.5 Discussion

During the process described above, many attempts were made to find the origin of the big difference in current measured in Midel and in air. Some of the possibilities explored along the way are presented and discussed in this section.

3.2.5.1 Leakage Current

The test cell is designed with a guard electrode to pick up any leakage current going around the edges of the sample. One proposed explanation for the high current measured were that some of this current was reaching the measuring cable and/or electrode. To get an indication of whether this hypothesis could be correct, a measurement was performed where the picoammeter was connected to the guard electrode, rather then the measurement electrode. The applied voltage was 7 kV. This gave a total current of 4.1×10^{-8} A. With such a high current going to the guard electrode, chances are good that some of it is being picked up by the measurement cable. The reason for the much greater effect with Midel present in the system is likely that the conductivity of the liquid is a factor 10^5 higher than the conductivity of air.

Then, a measurement was done with a cable without any screen, giving a current one order of magnitude higher than with a shielded cable, providing an indication of what the size of the leakage current to the measurement cable could be, see measurement no. 10 in Table 3.2. This gave an increase in measured current of one order of magnitude, contributing to the idea that leakage current is causing the problem, and that shielding of the cable is important to avoid picking up current from the surrounding liquid.

3.2.5.2 Potential Difference Between Guard and Measure Electrode

According to the manufacturer, the picoammeter in use has a voltage burden of maximum 200 µV [18]. This means that a potential drop of up to 200 µV can occur across the instrument, resulting in an equivalent drop across the gap between the guard and measure electrode. A current could then run between the guard and measure electrode, limited by the resistance of the material filling the gap. With air, the resistance is sufficiently high for the current to be insignificant. With Midel, the resistance is measured to $8 \times 10^{9}\,\Omega$ when applying 100 V. Using Equation (2.1), the expected current with the full voltage burden is calculated to $I_{burden} = 2.5 \times 10^{-14}\,\text{A}$. This value is considerably lower than what is measured, and can therefore not be the full explanation. It should however be taken into account when considering errors in the measurements. A solution that would reduce this contribution to error would be to increase the resistance between the two electrodes, filling the gap with a material of higher volume resistivity.

3.2.5.3 Difference in Effective Electrode Area

The measure electrode is a hollow cylinder with a cross sectional area of $A_m = 5.2 \times 10^{-4}\,\text{m}^2$. For measurements in air and with no aluminium coating on the sample, this will be the effective electrode area. With Midel present in the system, filling the volume within the measure electrode, the effective electrode area will increase, due to the high conductivity of Midel compared to air. As illustrated in Figure 3.16, some of the current going through the sample in the center may go through the liquid and reach the measure electrode, increasing the measured current. In the worst case, we can imagine the Midel-filled electrode acting as an electrode with effective area equivalent to a solid electrode of the same diameter. With the current in a plane parallel electrode configuration being proportional to the electrode area (Equation (2.1)), this can increase the measured current by a factor 2.

However, the current measured in Midel is 2–3 orders of magnitude higher than the current measured in air, that is, a factor 100–1000 It can therefore be concluded that although the increase in electrode area might have a considerable effect, it can not explain the increase in current alone. Moreover, as seen from measurement no. 7 (Table 3.2), the same effect is also seen after applying an aluminium coating on the PTFE sample, giving an approximately equal electrode area for measurements in both air and Midel.

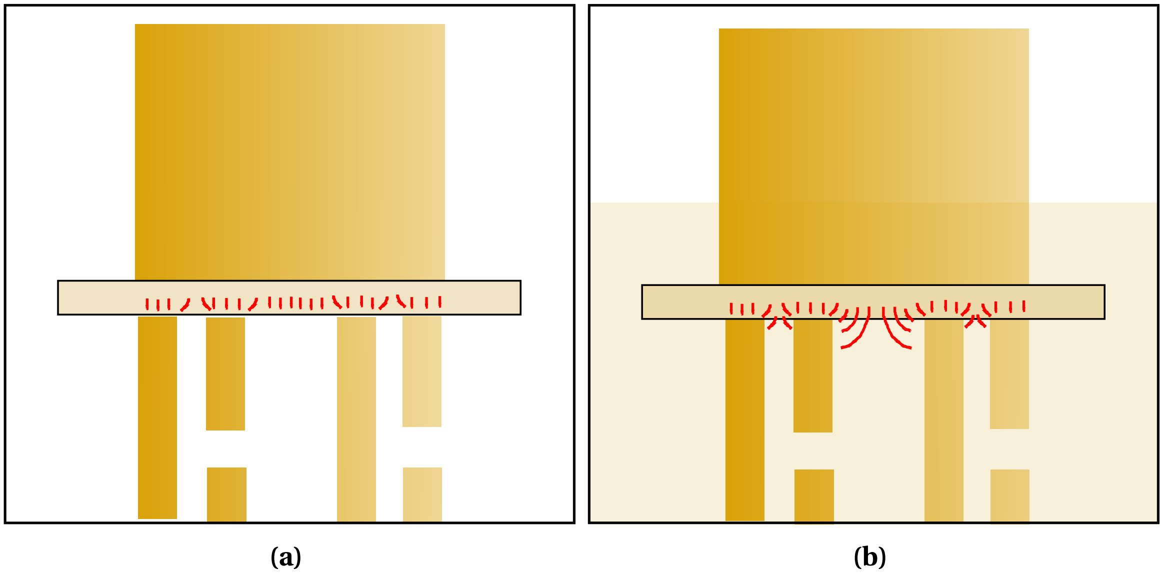

Figure 3.16: An illustration of how current (red) going through the center of the sample could reach the measure electrode by going through the Midel. Here, no aluminium electrodes are applied on the sample.

3.2.5.4 Different levels of Midel in the container

Measurements no. 7, 8 and 9 in Table 3.2 are done with the same setup, but with different amounts of Midel in the container, see Figure 3.17. A big difference is seen between measurement no. 8 and 9, with Midel covering the measuring cable and not covering the measuring cable, respectively. With no Midel above the cable, the measured current is at the same level as for measurements in air. Whether Midel covers the sample or not seems to be of less importance, as seen when comparing measurement no. 7 and 8. It is also interesting that the measured current appears to be the same, independent of whether Midel is in contact with the high voltage electrode or not. However, Midel is removed from the container with a syringe, and no parts of the setup are cleaned so that a thin layer of Midel may still be present on the sample and the high voltage electrode. This could account for an equally high leakage current for measurements no. 7 and 8. Why the same effect is not seen when the Midel level is lowered to below the measurement cable is not clear. Again, the measurement cable appears to be the key factor for understanding/explaining the observed phenomena.

One can imagine that if leakage current reached the measure electrode directly, the measured current would be proportional on the area of the electrode covered in Midel. For these measurements, the level of Midel in the container is lowered by approximately 2 cm each time, and hence reducing the covered electrode area linearly. A similar linear reduction is not seen in the measured current, substantiating the idea that the problem lies with the measuring cable.

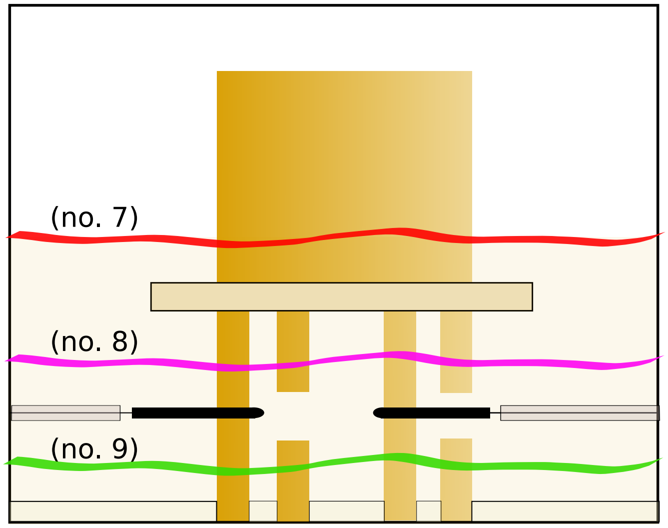

Figure 3.17: An illustraion showing how much Midel was in the container for measurements no. 7, 8 and 9 in Table 3.2.

3.2.6 Preliminary Measurements on PEEK in Midel

The solution with the measuring cable connected under the test cell, described in iteration 6, Section 3.2.4, gave a measured current of 8.40×10^{-13} A (Measurement no. 13, Table 3.2). For PEEK, the current measured in air is 8.03×10^{-12} A. A bias current level around 1 pA should then be sufficiently low for measuring changes in PEEK due to Midel.

To demonstrate the functionality of the final setup a series of measurements was conducted on both PTFE and PEEK. New, dry samples were used, prepared as described in Section 3.1.1 and Section 3.2.1. The Midel in the cointaier was replaced with new Midel, dried as explained in Section 3.1.1. The test cell was assembled after the container was filled with Midel to ensure that no air is trapped under the sample, see Section 3.2.2. The temperature was set to 90 °C and the measurement procedure described in Section 3.1.3.1 was followed. The results are presented and discussed in Chapter 4.

3.3 The High Pressure Setup

Another central part of the work carried out this semester has been the construction of an experimental setup for measuring the effect of high pressure on the electrical properties of PEEK. This section explains some of the choices made when designing the setup. A sketch of the setup is shown in Figure 3.18. It closely resembles the setup presented in Section 3.1. The main difference is that the sample and test cell will be placed in a pressure vessel, see Figure 3.19a. This way, a pressure of up to 300 bar can be applied to the sample and the temperature set to the desired level.

The vessel is filled with Midel. The process described above, reducing the noise from Midel, is therefore highly relevant also for this setup. In addition, a proper characterization of the effect of Midel on PEEK at atmospheric pressure is essential to be able to distinguish the effect of pressure from the effect of Midel. This way, the two parts of the project are closely related.

Using Midel to pressurize the sample gives a great advantage when it comes to safety during the tests. As the liquid is nearly incompressible, the fallout of a leakage or damage to the pressure vessel would be far less severe compared to if the vessel was filled with air.

Figure 3.18 also shows the measuring circuit being used for conductivity measurements. When dielectric response measurements are to be done, a dielectric spectroscopy instrument is connected through the box (2) in the figure, as seen in Figure 3.19b.

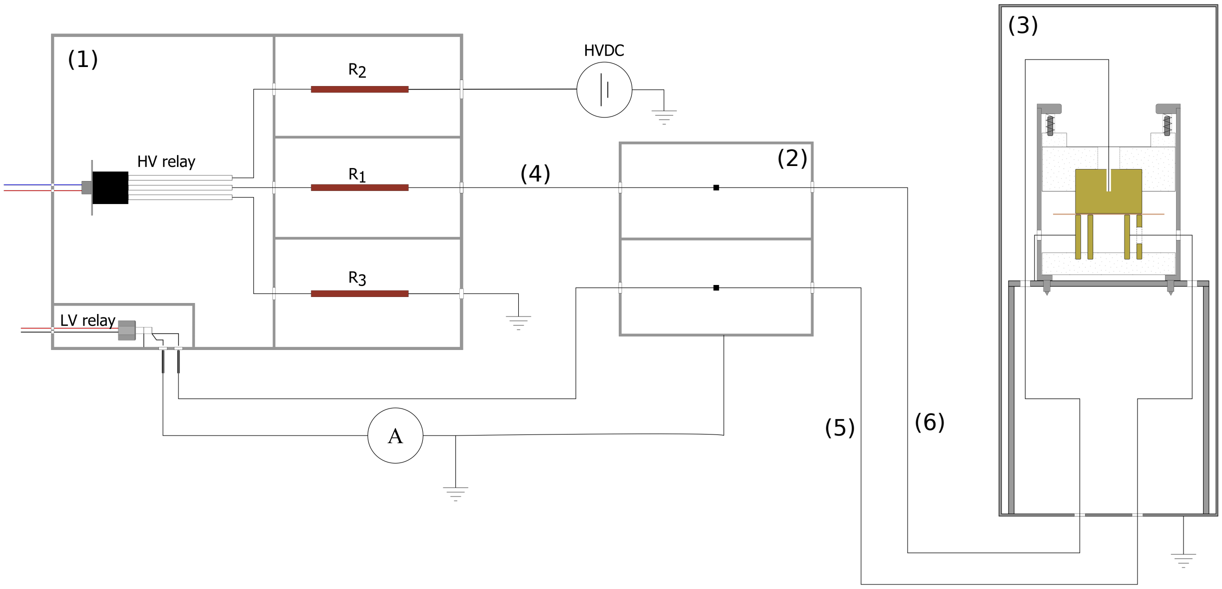

Figure 3.18: The setup built for conductivity and dielectric response measurements on PEEK in Midel at elevated pressures. Box (1) contains the high voltage, the low voltage relay and the resistors $R_1 = 50\,\text{k}\Omega$, $R_2 = 50\,\text{M}\Omega$ and $R_3 = 10\,\text{k}\Omega$, used during concuctivity measurements. The grounded box (2) screens the kables where the Novocontrol can be connected for dielectric response measurements. (3) is the pressure vessel containing the test cell with the sample. Cables (4), (5) and (6) are the miniature cables with copper tape.

3.3.0.1 Measuring Cable and High Voltage Cable

The cables going into the pressure vessel, applying the voltage across and picking up the current going through the sample, are XLPE miniature cables, chosen for the high resistance to partial discharges.

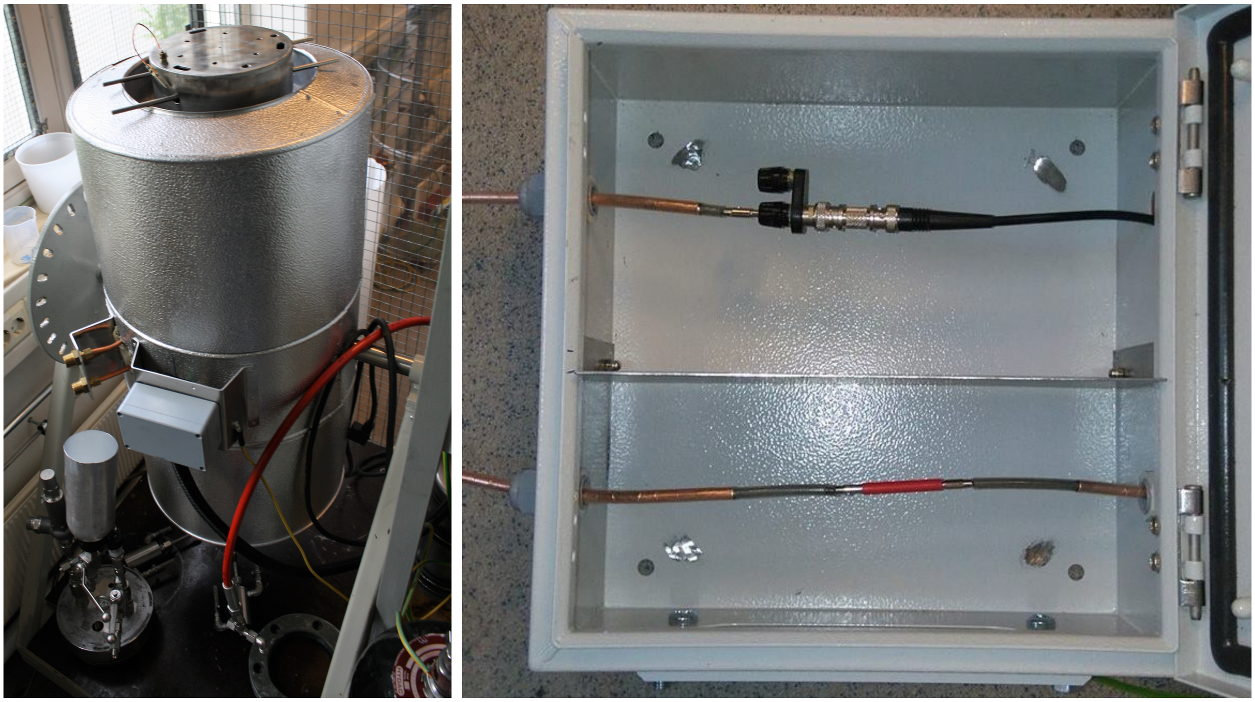

(a) The pressure vessel. Item (3) in Figure 3.18.

(b) The metal box shielding the cables where the Novocontrol instrument can be connected for dielectric response measurements. Item (2) in Figure 3.18.

(c) The XLPE miniature cables connecting the test cell electrodes to the picoammeter and high voltage source. Copper tape and a PTFE heatshrink tube is applied to reduce the exposure to Midel inside the pressure vessel and to ensure a conducting outer cable screen. Items (4), (5) and (6) in Figure 3.18.

Figure 3.19: Details from the high pressure setup.

However, this quality may be affected by the Midel filling the vessel. Tests conducted during summer 2016 found that this cable type absorbs Midel, causing an increase in the resistance of the outer semi-conducting screen of the cable[20]. The increase in resistance was significant enough to prevent the semi-conducting layer from acting as a screen. To counteract the effect from absorbed Midel, a copper tape with electrical conducting glue is wrapped around the full length of the cable. Then, a PTFE heat-shrink tube was applied, see Figure 3.19c. This solution will reduce the exposure of the cable to Midel, but will not be completely sealed. The copper tape is therefore needed to ensure a conducting cable screen.

Chapter 4

Results and Discussion

All results presented in this chapter are from measurements of dielectric response in time domain conducted at 90 °C. First, some general remarks about the collected data is presented. Then, the results from preliminary measurement series conducted at PTFE in Midel and on PEEK in Midel are presented and compared to results from measurements in air.

4.1 Dielectric response in time domain

As explained in Section 3.1.3.1, the dielectric response of a material in time domain is found by applying a DC step voltage across a sample and measure the current through it. An example of the measured current from one such measurement on PEEK in air is plotted in Figure 4.1. First, the noise is measured for 15 minutes with no voltage applied. Then, an electric field is applied and the sum of the polarization current and DC current is measured. When the field is removed, the depolarization current is measured. The shape closely resembles the theoretical shape of the current through a material with one relaxation mechanism, sketched in Figure 2.1.

When the electric field is applied and removed, the input of the picoammeter is grounded for one second. The spikes due to immediate polarization mechanisms are therefore nok measured. The part of the polarization- and depolarization currents seen in the figure is due to slower relaxation mechanisms in the material. Also, the decay is not perfectly exponential, indicating that more than one relaxation mechanism contributes to the measured current.

After application of the field, the current relaxes towards a steady level, with contributions from both leakage current going around the edges of the sample and current through the bulk of the material. To be

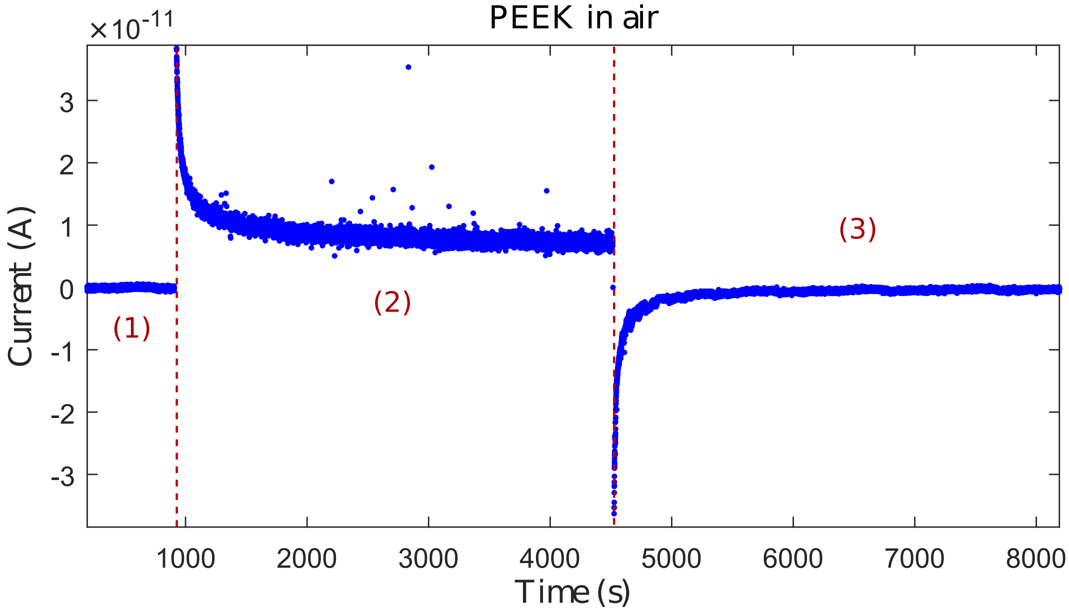

Figure 4.1: Example: The raw signal from a measurement on PEEK in air. An electric field of 28 kV/mm is applied at $t_1 = 900\,\mathrm{s}$ and removed at $t_2 = 4500\,\mathrm{s}$. (1) is the noise measurement, (2) is the polarization current pluss DC current and (3) is the depolarization current.

able to calculate the conductivity of the material from this value, the leakage current contribution must be negligible compared to the current through the material.

A median filter is used to remove the most extreme noise from the data. This is done by iterating over the signal in intervals of specified length. For each interval, only the median value is kept. The noise we seek to filter out mainly consists of single ponts. Therefore, a short interval can be used, choosing 5 points in this case. Figure 4.2 shows plots of the measured polarization currents for PTFE in air and in Midel. Both the raw signal and filtered signal is plotted, demonstrating the effect of the filter.

When comparing signals from measurements in Midel and in air, the noise was generally bigger in Midel in the part of the signal for which voltage was applied across the sample. An example of this is seen in Figure 4.2.

4.2 Proof-of-concept Measurements

To demonstrate the functionality of the final experimental setup, measurements were performed on dry PTFE and dry PEEK submerged in dry Midel at 90 °C. The final setup and the measurement procedure is described in Section 3.2.6.

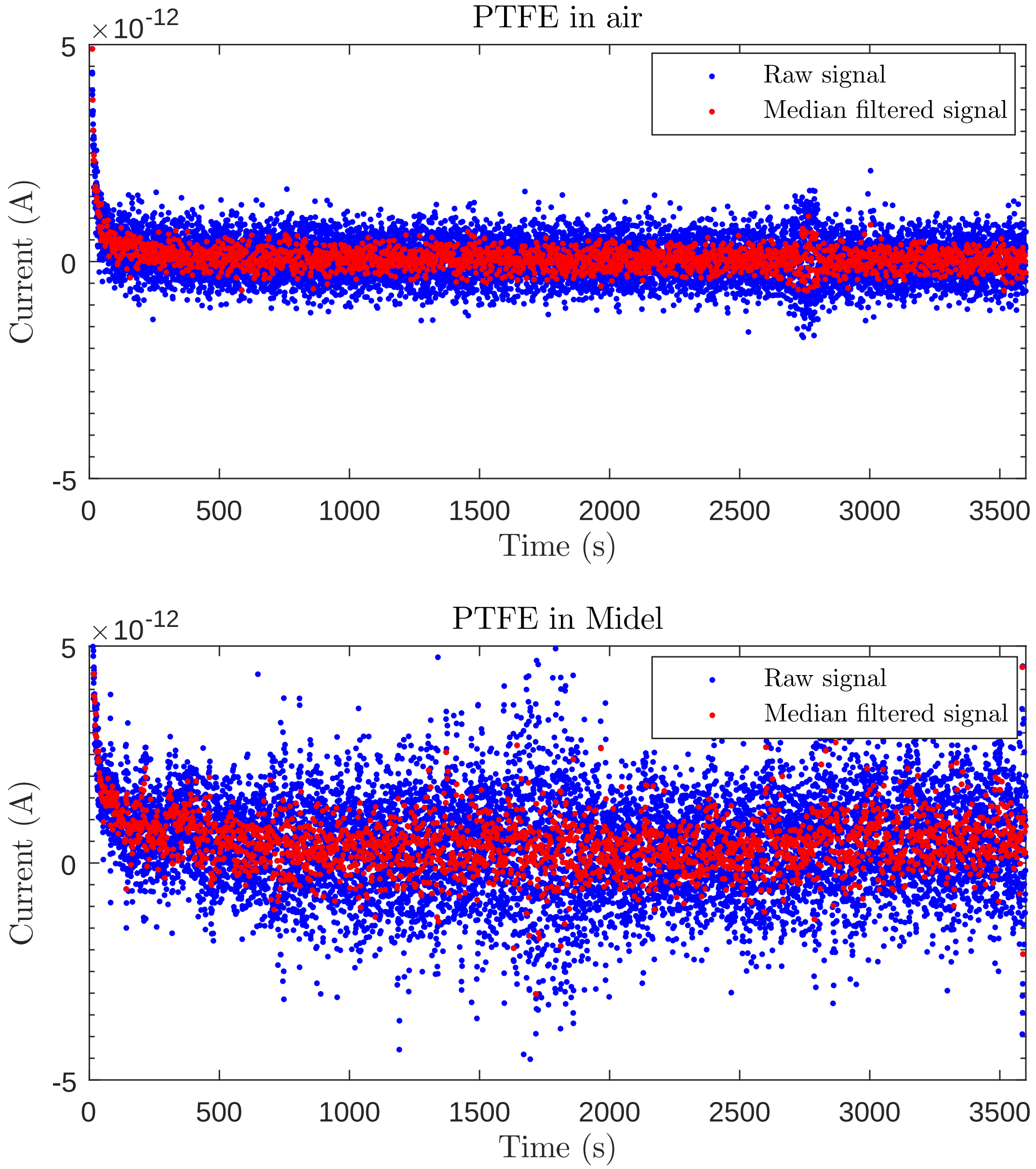

Figure 4.2: Example: The raw signal and median filtered signal from measurements at 7 kV on PTFE in air (top) and in Midel (bottom). An average of the noise measurement is subtracted.

4.2.1 PTFE in Air and in Midel

In total, eleven measurements on PTFE in air was performed during the process of developing the setup. An average value of 1.92×10^{-13} A is calculated at 7 kV. Because the measured current seems to be unaffected by the changes made to the experimental setup, varying little from iteration to iteration, this value will be used to compare measurements on PTFE in air and in Midel.

Figure 4.3 shows the total current calculated from measurements on PTFE in Midel. Measurements on 5 kV/mm and 6 kV/mm are missing due to problems with the automated measurement procedure. From this plot, the measured current seems to be mostly independent of the applied electrical field. In that case, comparing to the measured current for PTFE in air, the bias current from Midel in the system can be considered constant at around 1 pA. While more measurements should be conducted before any conclusions are drawn, this will be assumed to be the systematic bias from Midel in the remainder of this report.

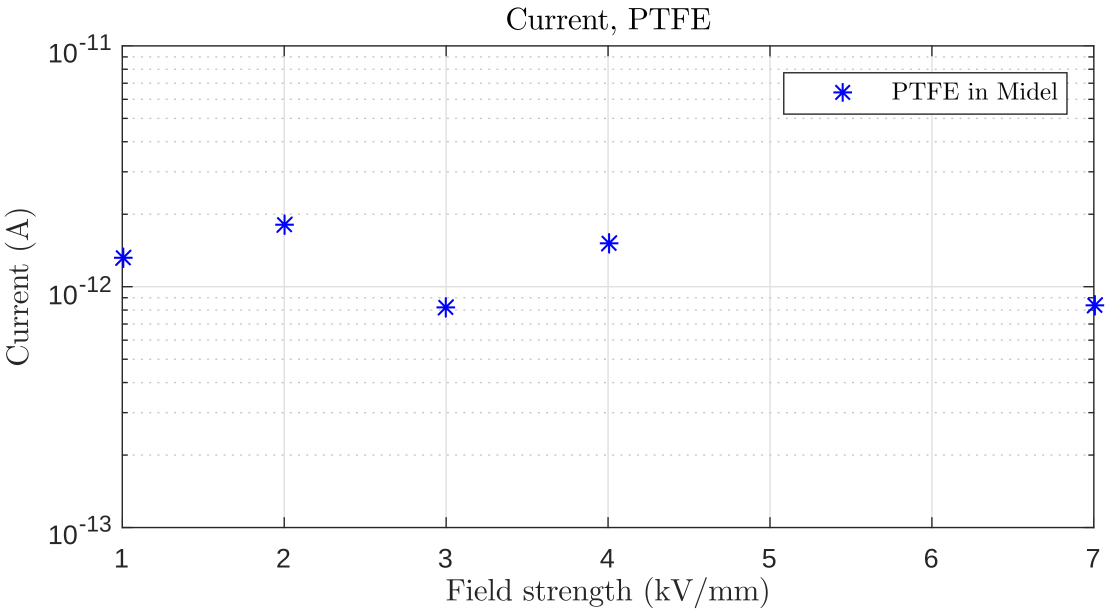

Figure 4.3: Current measurement results, PTFE in Midel, conducted at 90 °C.

4.2.2 PEEK in Air and in Midel

The results from measurements on PEEK immersed in Midel are plotted in Figure 4.4. For comparison, results from measurements on PEEK in air are plotted in the same figure, conducted during summer 2016[17].

The measured currents in Midel are in the order of 10^{-11} A, well above the bias current from Midel, found to be in the order of 10^{-12} A. Consequently, Midel affecting the system can not explain the big difference in the measured current for measurements on PEEK in Midel and in air. The observed phenomena seems therefore likely to be due to changes in the material itself.

The conductivity was calculated from the current measurements on PEEK, using Equation (2.1) and

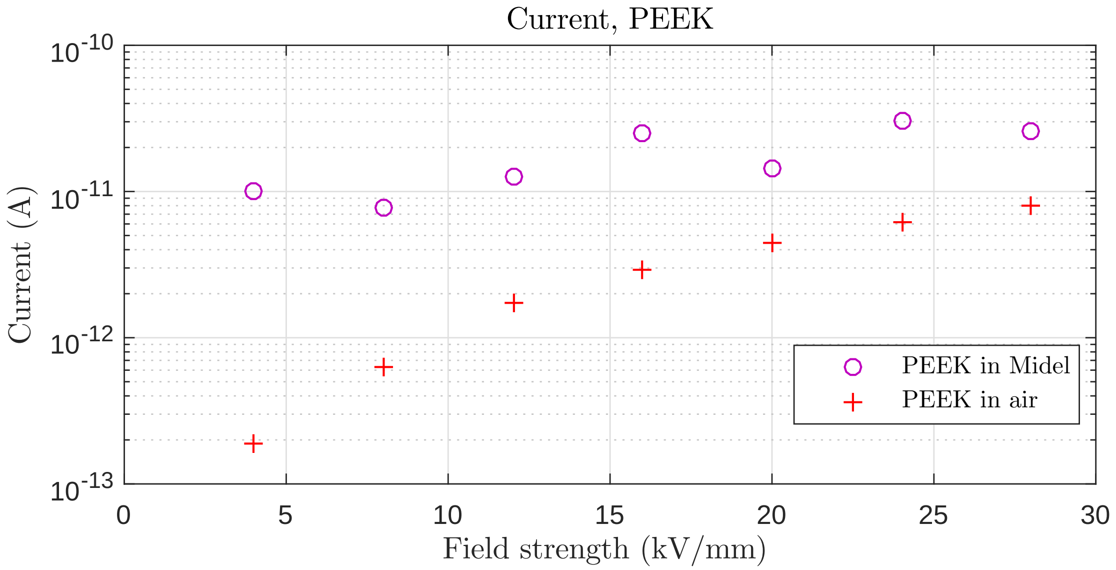

Figure 4.4: Current measurement results, PEEK in air and in Midel, conducted at 90 °C.

the sample geometry stated in Section 3.1.1. The result is plotted in Figure 4.5. These preliminary measurements indicates a significant increase in the conductivity of PEEK when immersed in Midel. In addition, a reduction in the field dependency of the conductivity is seen.

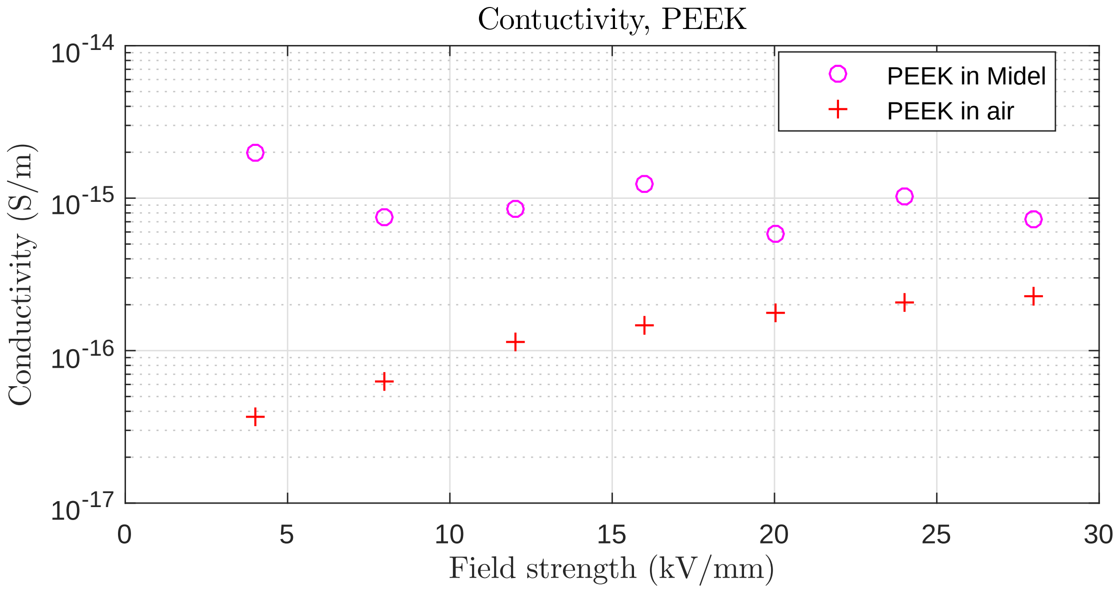

Figure 4.5: Conductivity of PEEK, calculated from current measurements plotted in Figure 4.4. Measurements conducted at 90 °C.

Chapter 5

Conclusion and Recommendations for Further Work

5.1 Summary and Conclusions

An experimental setup has been developed for measurements of dielectric response in time domain and in frequency domain on a dielectric material immersed in a dielectric liquid. A setup for measurements in air was taken as a starting point and adapted to work for measurements on a sample of PEEK immersed in Midel 7131. When first introducing Midel to the system, a high bias current was measured, making it impossible to distinguish the effect from Midel on the measurement system and on the sample itself. The main hypothesis for the origin of the bias current was that leakage current was going around the edges of the sample, through the liquid, and reaching the measuring cable or the measure electrode. The main adjustments to the setup was to improve the guarding and to improve the measuring cable screen. Several iterations were tried, resulting in a setup where the measuring cable was attached to the measure electrode from underneath the test cell. This way, the bias current was reduced by 3 orders of magnitude to approximately 1 pA, a sufficiently low level for measurements of conductivity on PEEK immersed in Midel.

Preliminary measurements on PEEK in Midel have been performed, providing a proof of concept and demonstrating the functionality of the setup. The results show that conductivity measurements on PEEK immersed in Midel 7131 are feasible with the developed setup. The results from the preliminary measurements, presented in Chapter 4, indicate that Midel increases the electric conductivity of PEEK and reduces the electric field dependence of the conductivity. The measured currents are in the order of

8×10^{-12}–3×10^{-11} A for PEEK in Midel and in the range 2×10^{-13}–8×10^{-12} A for PEEK in air. The 1 pA bias, arising from Midel affecting the measurement setup, can not explain the big difference, and hence, the effect seems likely to be due to changes in the material itself.

5.2 Recommendations for Further Work

The preliminary results from measurements on PEEK immersed in Midel strongly encourages further investigation of the observed phenomena. In further work, the following points should be considered.

- More measurements should be conducted on PEEK immersed in Midel, also at other temperatures, to provide a statistical basis for analyzing the effect of Midel on PEEK. Polarization mechanisms and relaxation times could be looked into in more detail.
- Measure the dielectric response in samples of PEEK which can be considered fully saturated with Midel, conditioned in Midel at different temperature for up to one year.
- More measurements should be conducted on PTFE to further characterize the bias current.
- Measurements on PEEK in air could be conducted with the new setup for comparison.
- The developed setup should be tested for measurements of dielectric response in frequency domain.
- Complete the setup for measurements of dielectric response at elevated pressures. Study the pressure dependency of the dielectric response in PEEK immersed in Midel.

Appendix A

Datasheet PEEK

Product Information

VESTAKEEP® 3300G

Medium-viscosity, unreinforced polyether ether ketone

VESTAKEEP 3300G is a medium-viscosity, unreinforced polyether ether ketone for injection molding and extrusion.

The semi-crystalline polymer features superior thermal and chemical resistance. Parts made from VESTAKEEP 3300G are self-extinguishing.

VESTAKEEP 3300G can be processed by common machines for thermoplastics.

We recommend a melt temperature between 360°C and 380°C during the injection molding process. The mold temperature should be within a range of 160°C to 200°C, preferably 180°C.

VESTAKEEP 3300G is supplied as granules in 25 kg boxes with moisture-proof polyethylene liners.

For information about processing VESTAKEEP 3300G, please follow the general recommendations in our brochure “VESTAKEEP Polyether Ether Ketone.“

Property		Test method		Unit	VESTAKEEP 3300G
		international	national		
Density	23°C	ISO 1183	DIN EN ISO 1183	g/cm^3	1.30
Tensile test		ISO 527-1	DIN EN ISO 527-1		
Stress at yield		ISO 527-2	DIN EN ISO 527-2	MPa	98
Strain at yield				%	5
Strain at break				%	25
Tensile modulus		ISO 527-1 ISO 527-2	DIN EN ISO 527-1 DIN EN ISO 527-2	MPa	3600
CHARPY impact strength		ISO 179/1eU	DIN EN ISO 179/1eU		
	23°C			kJ/m^2	N 1)
	-30°C			kJ/m^2	N 1)
CHARPY notched impact strength		ISO 179/1eA	DIN EN ISO 179/1eA		
	23°C			kJ/m^2	6 C 1)
	-30°C			kJ/m^2	6 C 1)
Vicat softening temperature		ISO 306	DIN EN ISO 306		
Method A	10 N			°C	335
Method B	50 N			°C	305
Linear thermal expansion		ISO 11359	DIN 53752		
	23-55°C				
longitudinal				$10^{-4}K^{-1}$	0.6
Relative permittivity		IEC 60250	DIN VDE 0303-T4		
	50 Hz				2.8
	1 MHz				2.8
Electric strength	K20/P50	IEC 60243-1	IEC 60243-1	kV/mm	16
Comparative tracking index		IEC 60112	IEC 60112		
Test solution A	CTI				200
	100 drops value				175
Volume resistivity		IEC 60093	DIN IEC 60093	Ohm · cm	10^{15}
Surface resistance		IEC 60093	DIN IEC 60093	Ohm	10^{14}
Melting range		ISO 11357			
DSC	2nd heating			°C	approx. 340
Melt volume-flow rate (MVR)		ISO 1133	DIN EN ISO 1133		
	380°C/5kg			$cm^3/10$ min	20
Flammability acc. UL94		IEC 60695	UL94		
	3.2 mm				V-0
Glow wire test		IEC 60695-2- 12/13	DIN EN 60695-2- 12/13		
GWIT	2 mm			°C	800
GWFI	2 mm			°C	960
Mold shrinkage		determined on 2 mm sheets			
	in flow direction	with film gate at rim		%	0.9
	in transverse direction	mold temperature 180°C, ISO 294-4		%	1.1

Pigmentation may affect values.

1) C = Complete break, incl. hinge break H
N = No break

Evonik Industries AG High Performance Polymers 45764 Marl Germany
Phone +49 2365 49-9878 E-mail evonik-hp@evonik.com
www.vestakeep.com

Appendix B

Datasheet MIDEL 7131

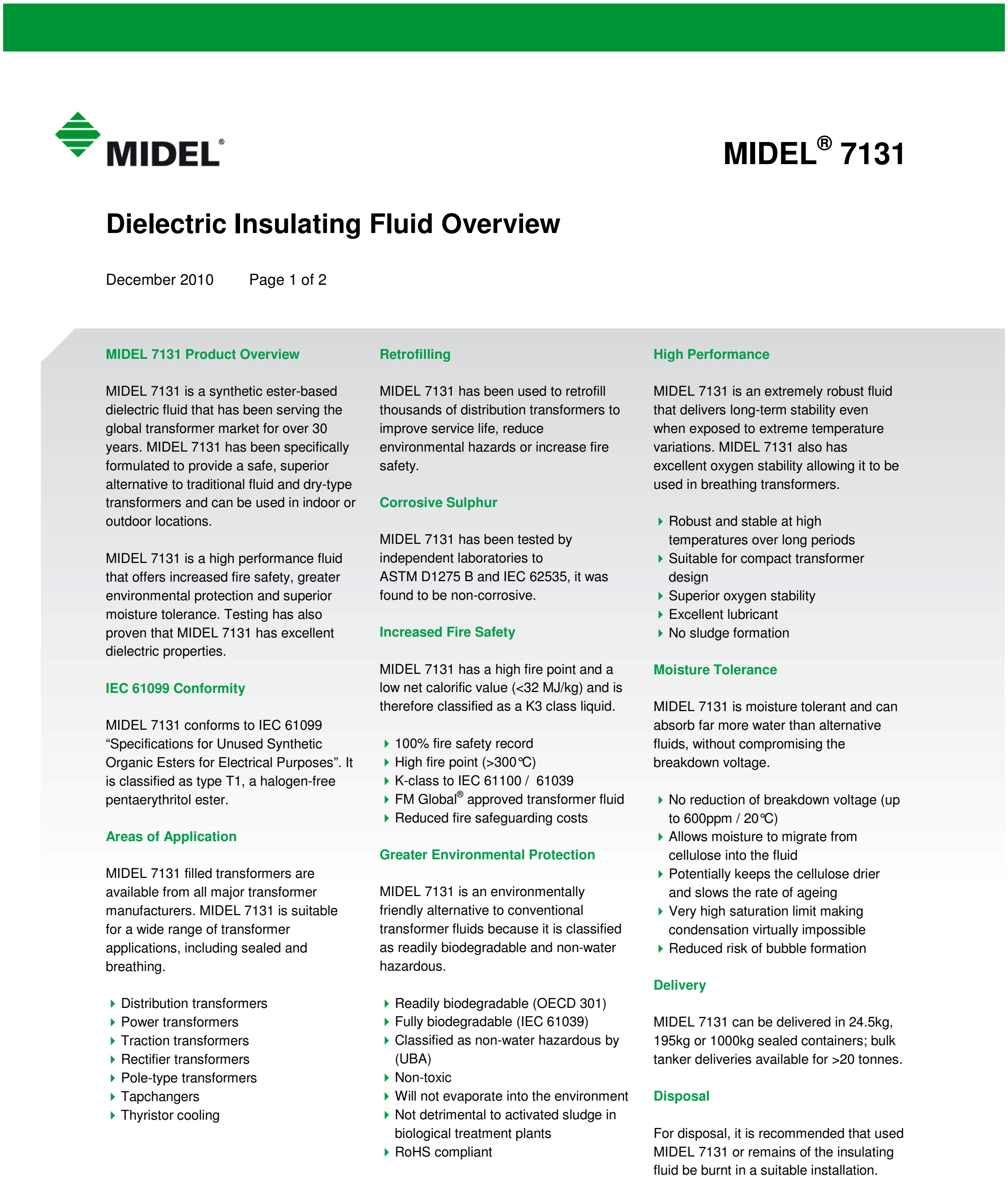

MIDEL®

MIDEL® 7131

Dielectric Insulating Fluid Overview

December 2010 Page 1 of 2

MIDEL 7131 Product Overview

MIDEL 7131 is a synthetic ester-based dielectric fluid that has been serving the global transformer market for over 30 years. MIDEL 7131 has been specifically formulated to provide a safe, superior alternative to traditional fluid and dry-type transformers and can be used in indoor or outdoor locations.

MIDEL 7131 is a high performance fluid that offers increased fire safety, greater environmental protection and superior moisture tolerance. Testing has also proven that MIDEL 7131 has excellent dielectric properties.

IEC 61099 Conformity

MIDEL 7131 conforms to IEC 61099 “Specifications for Unused Synthetic Organic Esters for Electrical Purposes”. It is classified as type T1, a halogen-free pentaerythritol ester.

Areas of Application

MIDEL 7131 filled transformers are available from all major transformer manufacturers. MIDEL 7131 is suitable for a wide range of transformer applications, including sealed and breathing.

- Distribution transformers
- Power transformers
- Traction transformers
- Rectifier transformers
- Pole-type transformers
- Tapchangers
- Thyristor cooling

Retrofilling

MIDEL 7131 has been used to retrofill thousands of distribution transformers to improve service life, reduce environmental hazards or increase fire safety.

Corrosive Sulphur

MIDEL 7131 has been tested by independent laboratories to ASTM D1275 B and IEC 62535, it was found to be non-corrosive.

Increased Fire Safety

MIDEL 7131 has a high fire point and a low net calorific value (<32 MJ/kg) and is therefore classified as a K3 class liquid.

- 100% fire safety record
- High fire point (>300℃)
- K-class to IEC 61100 / 61039
- FM Global® approved transformer fluid
- Reduced fire safeguarding costs

Greater Environmental Protection

MIDEL 7131 is an environmentally friendly alternative to conventional transformer fluids because it is classified as readily biodegradable and non-water hazardous.

- Readily biodegradable (OECD 301)
- Fully biodegradable (IEC 61039)
- Classified as non-water hazardous by (UBA)
- Non-toxic
- Will not evaporate into the environment
- Not detrimental to activated sludge in biological treatment plants
- RoHS compliant

High Performance

MIDEL 7131 is an extremely robust fluid that delivers long-term stability even when exposed to extreme temperature variations. MIDEL 7131 also has excellent oxygen stability allowing it to be used in breathing transformers.

- Robust and stable at high temperatures over long periods
- Suitable for compact transformer design
- Superior oxygen stability
- Excellent lubricant
- No sludge formation

Moisture Tolerance

MIDEL 7131 is moisture tolerant and can absorb far more water than alternative fluids, without compromising the breakdown voltage.

- No reduction of breakdown voltage (up to 600ppm / 20℃)
- Allows moisture to migrate from cellulose into the fluid
- Potentially keeps the cellulose drier and slows the rate of ageing
- Very high saturation limit making condensation virtually impossible
- Reduced risk of bubble formation

Delivery

MIDEL 7131 can be delivered in 24.5kg, 195kg or 1000kg sealed containers; bulk tanker deliveries available for >20 tonnes.

Disposal

For disposal, it is recommended that used MIDEL 7131 or remains of the insulating fluid be burnt in a suitable installation.

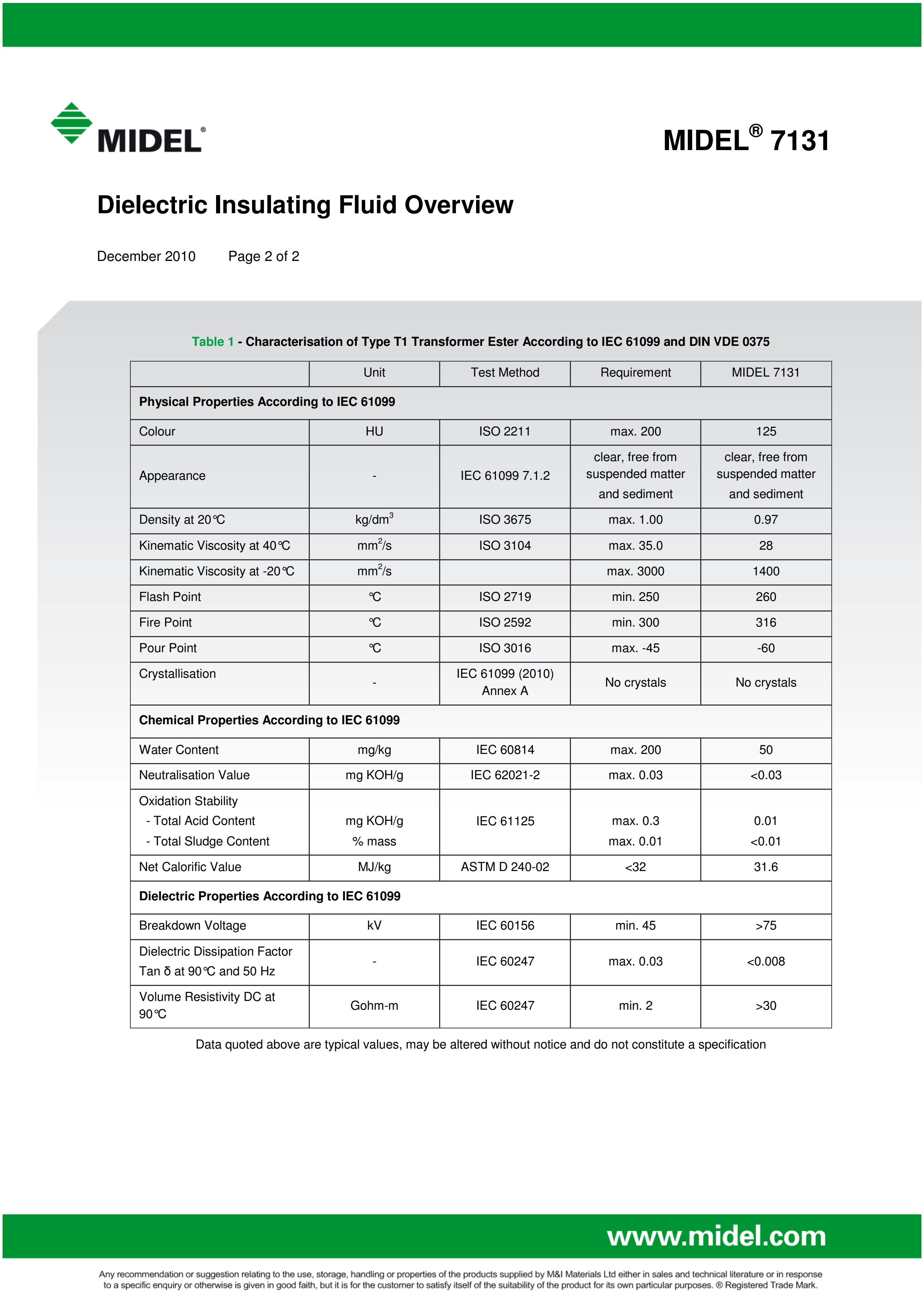

MIDEL® 7131

Dielectric Insulating Fluid Overview

December 2010 Page 2 of 2

Table 1 - Characterisation of Type T1 Transformer Ester According to IEC 61099 and DIN VDE 0375

	Unit	Test Method	Requirement	MIDEL 7131
Physical Properties According to IEC 61099				
Colour	HU	ISO 2211	max. 200	125
Appearance	-	IEC 61099 7.1.2	clear, free from suspended matter and sediment	clear, free from suspended matter and sediment
Density at 20°C	kg/dm^3	ISO 3675	max. 1.00	0.97
Kinematic Viscosity at 40°C	mm^2/s	ISO 3104	max. 35.0	28
Kinematic Viscosity at -20°C	mm^2/s		max. 3000	1400
Flash Point	°C	ISO 2719	min. 250	260
Fire Point	°C	ISO 2592	min. 300	316
Pour Point	°C	ISO 3016	max. -45	-60
Crystallisation	-	IEC 61099 (2010) Annex A	No crystals	No crystals
Chemical Properties According to IEC 61099				
Water Content	mg/kg	IEC 60814	max. 200	50
Neutralisation Value	mg KOH/g	IEC 62021-2	max. 0.03	<0.03
Oxidation Stability - Total Acid Content - Total Sludge Content	mg KOH/g % mass	IEC 61125	max. 0.3 max. 0.01	0.01 <0.01
Net Calorific Value	MJ/kg	ASTM D 240-02	<32	31.6
Dielectric Properties According to IEC 61099				
Breakdown Voltage	kV	IEC 60156	min. 45	>75
Dielectric Dissipation Factor Tan δ at 90°C and 50 Hz	-	IEC 60247	max. 0.03	<0.008
Volume Resistivity DC at 90°C	Gohm-m	IEC 60247	min. 2	>30

Data quoted above are typical values, may be altered without notice and do not constitute a specification

www.midel.com

Bibliography

[1] T. G. Aakre, T. A. Ve, and Ø. L. Hestad. Conductivity and permittivity of midel 7131: effect of temperature, moisture content, hydrostatic pressure and electric field. *IEEE Transactions on Dielectrics and Electrical Insulation*, 23(5):2957–2964, October 2016.

[2] Jostein Danielsen Kvitvang. Bulk conductivity and dielectric response of PEEK and Midel 7131. Summer internship report, unpublished.

[3] D. K. Das-gupta and K. Doughty. Dielectric and conduction processes in polyetherether ketone (peek). *IEEE Transactions on Electrical Insulation*, EI-22(1):1–7, Feb 1987.

[4] Tony Blythe and David Bloor. *Electrical Properties of Polymers*. Cambridge Solid State Science Series. Cambridge University Press, 2 edition, 2005.

[5] M. Ieda. Electrical conduction and carrier traps in polymeric materials. *IEEE Transactions on Electrical Insulation*, EI-19(3):162–178, June 1984.

[6] L.A. Dissado and J.C. Fothergill. *Electrical Degradation and Breakdown in Polymers*. IEE materials & devices series. P. Peregrinus, 1992.

[7] I. Rubinstein. *Electro-Diffusion of Ions*. Studies in Applied Mathematics. Society for Industrial and Applied Mathematics, 1990.

[8] Charles Kittel. *Introduction to Solid State Physics*. John Wiley & Sons, Inc., New York, 6th edition, 1986.

[9] K J Less and E G Wilson. Intrinsic photoconduction and photoemission in polyethylene. *Journal of Physics C: Solid State Physics*, 6(21):3110, 1973.

[10] G. Teyssedre and C. Laurent. Charge transport modeling in insulating polymers: from molecular to macroscopic scale. *IEEE Transactions on Dielectrics and Electrical Insulation*, 12(5):857–875, Oct 2005.

[11] A.L. Kovarski. *Molecular Dynamics of Additives in Polymers.* New concepts in polymer science. Taylor & Francis, 1997.

[12] Matt Petrowsky and Roger Frech. Temperature dependence of ion transport: The compensated arrhenius equation. *The Journal of Physical Chemistry B*, 113(17):5996–6000, 2009. PMID: 19338318.

[13] Erling Ildstad. *TET4160 - High Voltage Insulation Materials.* Department of Electrical Power Engineering, NTNU, 2016.

[14] K.C. Kao. *Dielectric Phenomena in Solids.* Elsevier Science, 2004.

[15] A.K. Jonscher. *Dielectric Relaxation in Solids.* Chelsea Dielectrics Press Limited, 1983.

[16] Vemund Kaurstad Mørk. Karakterisering av silikongummi for HVDC subsea-konnektorer. Master's thesis, Norges teknisk-naturvitenskapelige universitet, NTNU, 7491 Trondheim, 2016.

[17] Elise Otterlei Brenne. Measurements of conductivity and dielectric response of PEEK submerged in Midel 7131. Summer internship report, unpublished.

[18] Low current measurements - application note series, number 1671, 2012. "[Online; accessed 25-October-2016]".

[19] Teflon ptfe - properties handbook, 2012. "[Online; accessed 05-September-2016]".

[20] Elise Otterlei Brenne. Resistivity measurements on semi-conducting screen of Midel-conditioned miniature cables by four-point method. Summer internship report, unpublished.